

Journal Pre-proof

Identification of novel non-nucleoside vinyl-stilbene analogs as potent norovirus replication inhibitors with a potential host-targeting mechanism

Dipesh S. Harmalkar, Sung-Jin Lee, Qili Lu, Mi Il Kim, Jaehyung Park, Hwayoung Lee, Minkyung Park, Ahrim Lee, Choongho Lee, Kyeong Lee



PII: S0223-5234(19)30885-2

DOI: <https://doi.org/10.1016/j.ejmech.2019.111733>

Reference: EJMECH 111733

To appear in: *European Journal of Medicinal Chemistry*

Received Date: 5 August 2019

Revised Date: 16 September 2019

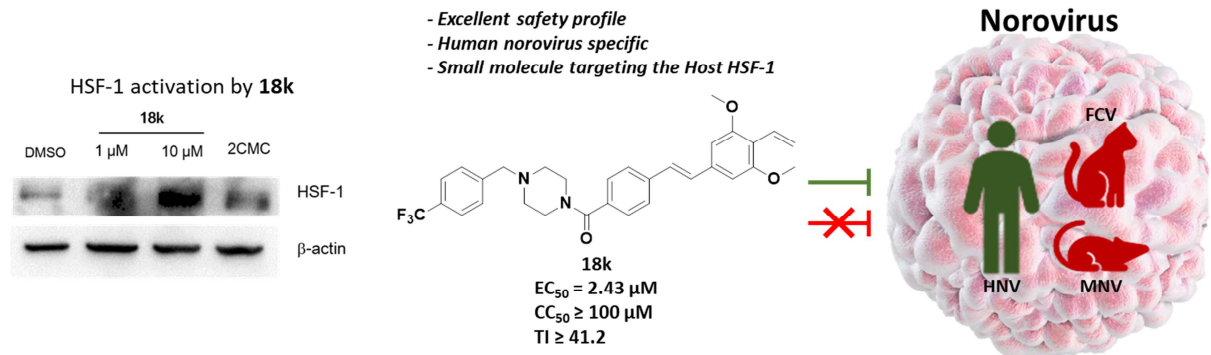
Accepted Date: 22 September 2019

Please cite this article as: D.S. Harmalkar, S.-J. Lee, Q. Lu, M.I. Kim, J. Park, H. Lee, M. Park, A. Lee, C. Lee, K. Lee, Identification of novel non-nucleoside vinyl-stilbene analogs as potent norovirus replication inhibitors with a potential host-targeting mechanism, *European Journal of Medicinal Chemistry* (2019), doi: <https://doi.org/10.1016/j.ejmech.2019.111733>.

This is a PDF file of an article that has undergone enhancements after acceptance, such as the addition of a cover page and metadata, and formatting for readability, but it is not yet the definitive version of record. This version will undergo additional copyediting, typesetting and review before it is published in its final form, but we are providing this version to give early visibility of the article. Please note that, during the production process, errors may be discovered which could affect the content, and all legal disclaimers that apply to the journal pertain.

© 2019 Published by Elsevier Masson SAS.

Graphical abstract



**Identification of Novel Non-Nucleoside Vinyl-Stilbene Analogs as
Potent Norovirus Replication Inhibitors with a Potential Host-
Targeting Mechanism**

Dipesh S. Harmalkar, Sung-Jin Lee, Qili Lu, Mi Il Kim, Jaehyung Park, Hwayoung Lee,
Minkyung Park, Ahrim Lee, Choongho Lee* and Kyeong Lee*

College of Pharmacy, Dongguk University-Seoul, Goyang, 10326, Republic of Korea

E-mail: choongholee@dongguk.edu; E-mail: kaylee@dongguk.edu

Abstract

Norovirus (NV), is the most common cause of acute gastroenteritis worldwide. To date, there is no specific anti-NV drug or vaccine to treat NV infections. In this study, we evaluated the inhibitory effect of different stilbene-based analogs on RNA genome replication of human NV (HNV) using a virus replicon-bearing cell line (HG23). Initial screening of our in-house chemical library against NV led to the identification of a hit containing stilbene scaffold **5** which on initial optimization gave us a vinyl stilbene compound **16c** ($EC_{50} = 4.4 \mu\text{M}$). Herein we report our structure-activity relationship study of the novel series of vinyl stilbene analogs that inhibits viral RNA genome replication in a human NV-specific manner. Among these newly synthesized compounds, several amide derivatives of vinyl stilbenes exhibited potent anti-NV activity with EC_{50} values ranging from 1 to 2 μM . A *trans*-vinyl stilbenoid with an appended substituted piperazine amide (**18k**), exhibited potent anti-NV activity and also displayed favorable metabolic stability. Compound **18k** demonstrated an excellent safety profile, the highest suppressive effect, and was selective for HNV replication via a viral RNA polymerase-independent manner. Its potential host-targeting antiviral mechanism was further supported by specific activation of heat shock factor 1-dependent stress-inducible pathway by **18k**. These results suggest that **18k** might be a promising lead compound for developing novel NV inhibitors with the novel antiviral mechanism.

Keywords: Norovirus, Inhibitors, Non-nucleoside, Vinyl-Stilbenes, HSF-1.

Journal Pre-proof

1. Introduction

Norovirus (NV) is a single-stranded positive-sense RNA (7.4–7.7 kb) virus belonging to the *Caliciviridae* family [1]. Human NV (HNV), in the genus NV, is the leading causative agent of epidemic gastroenteritis worldwide. NV infections can occur year round with very high morbidity and mortality in immunocompromised patients, young children, and older people [2,3]. HNVs are extremely stable in the environment, highly contagious, and generally transmitted via the fecal-oral route upon contamination of food products, water, or fomites [4]. According to a Centers for Disease Control and Prevention survey, NV causes approximately 200,000 deaths annually worldwide, and every year is estimated to cost \$60 billion worldwide due to healthcare costs and lost productivity [5].

NVs are phylogenetically divided into six genogroups (GI–GVI). HNV belongs to genogroup II (GII) and genotype 4 (GII.4), accounting for many of the global outbreaks. The NV genome consists of three open reading frames (ORF1–3). ORF1 encodes a large 200 kDa polyprotein that is cleaved by the virally encoded protease (NS6) to produce six nonstructural proteins. Among these nonstructural proteins, the viral protease (NS6) and RNA-dependent RNA polymerase (RdRp, NS7) play a critical role in viral RNA genome replication and hence have been attractive targets for discovering NV-specific therapeutics [6,7]. X-ray crystal structures of these proteins have provided a much-needed platform for the design and identification of small molecule NV inhibitors [8]. They include a peptidomimetic protease (NS6) inhibitor (rupintravir), nucleoside RdRp (NS7) inhibitors (2'-(2'-C-methylcytidine (2CMC) and ribavirin) and non-nucleoside RdRp (NS7) inhibitors (suramin and pyridoxal-5-phosphate-6-(2-naphthylazo-6-nitro-4,8-disulfonate tetrasodium salt (PPNDS)) (Fig. 1) [9-12].

To date, there have been no specific drugs or vaccines to treat NV infections; thus, there is a pressing need to develop effective anti-NV therapeutics. CMX521 is the first nucleoside in clinical development for the treatment and prevention of NV, which was developed by Chimerix. CMX521 is active *in vitro* against all strains of NVs tested to date and has a promising safety profile with high safety margins for human exposure [13]. In addition, the non-nucleoside drug nitazoxanide has demonstrated efficacy against NV infection in clinical trials. However, the exact mode of action of nitazoxanide against NV remains elusive (Fig. 1) [14,15].

Insert Figure 1

Phytochemicals such as curcumin and resveratrol have displayed antiviral effects against NV when evaluated using murine norovirus (MNV) and feline calicivirus (FCV) as surrogate models for NV biology. However, neither of these phytochemicals displays a strong inhibitory effect on HNV replication [16]. Very few reports are available on stilbene analogs with anti-NV activity. We have recently accomplished total synthesis of stilbene-based natural product gramisilbenoids A (**1**), B (**2**), and C (**3**) [17]. As part of our drug development program, our in-house chemical library containing these natural products and their synthetic analogs (**4–6**) were evaluated for different biological assays including anti-NV activity (Fig. 2). Among them, stilbenoid **5** with a vinyl moiety exhibited moderate inhibitory activity against NV replication. Considering **5** as a hit, derivatives of this compound were synthesized to perform a structure-activity relationship (SAR) study. Here, we report the design, synthesis, and biological activity of non-nucleoside stilbene-based NV replication inhibitors.

Insert Figure 2

2. Results and discussion

2.1 Chemistry

A series of vinyl stilbene analogs were synthesized as depicted in Schemes 1–4. The benzyl bromides **7a,b** on Arbuzav reaction gave phosphonate esters **8a,b** which underwent HWE olefination in the presence of NaH as a base with corresponding aldehydes to give selectively (*E*)-bromostilbenes **9a,b**. Compounds **9a,b** on Stille coupling yielded vinyl stilbenes **10a,b**, following the previous reports [17]. Compound **11** bearing hydroxyl ethyl moiety was synthesized from compound **10a** via the hydroboration-oxidation reaction. Additionally, (*E*)-stilbenes **12a,b** were synthesized using a synthetic route similar to **9a,b** (Scheme 1).

Insert Scheme 1

Similarly, (*E*)-stilbenes **15a–f** were synthesized from phosphonate esters **14a–f** and 4-bromo-3,5-dimethoxybenzaldehyde using HWE olefination. The ester group was hydrolyzed during HWE olefination to give acid analog **15f**, which was again methylated using MeI in the presence of K₂CO₃ to yield **15g**. Furthermore, Stille coupling on **15a–e** and **15g** afforded vinyl stilbenes **16a–e** and **16g**, respectively. The vinyl stilbene acid analog **16f** was obtained by hydrolysis of **16g** using LiOH (Scheme 2).

Insert Scheme 2

Compound **16f** on esterification with commercially available benzyl bromides in the presence of K₂CO₃ yielded ester derivatives **17a–d** (Scheme 3). The amide analogs **18a–m** were

synthesized from **16f** by coupling various amines under standard coupling conditions (Scheme 3).

Insert Scheme 3

To synthesize the *cis*-analogue **24a**, Wittig salt **19** was prepared from methyl 4-(bromomethyl)benzoate (**13f**) using PPh₃ and toluene as the solvent [18]. The obtained salt **19** was subjected to the Wittig reaction with 4-bromo-3,5-dimethoxybenzaldehyde in the presence of NaH to give both the (*E*)- (**15g**) and (*Z*)- (**20**) isomers in a 1:1 ratio, which were separated using column chromatography and confirmed by NMR studies. Pd/C hydrogenation on **20** provided saturated compound **21**. Stille coupling on compounds **20** and **21** afforded vinyl stilbenes **22a,b**. Basic hydrolysis to obtain **23a,b** and succeeding the amide coupling reaction with [4-(Trifluoromethyl)benzyl]piperazine in the presence of HATU yielded desired compounds **24a,b**. (Scheme 4).

Insert Scheme 4

2.2 Structure-Activity Relationship Studies

In search of more potent and efficient NV inhibitors, we evaluated the inhibitory effect of different stilbene-based analogues on the RNA genome replication by using a human NV replicon-bearing cell line (HG23), which is the only available in vitro human NV screening tool due to the inability to culture infectious NV in vitro. 2CMC was used as a reference compound. Initial screening of the compounds suggested that gramistilbenoid C (**3**), and intermediates **4** and **6** did not inhibit NV replication; however, vinyl stilbene **5** inhibited more than half of NV replication at 10 μ M (Table 1). Based on these results, the SAR study of gramistilbenoids was approached in a systematic manner in which the molecule was divided into four regions, as shown in Fig. 3.

Insert Figure 3

To improve anti-NV activity, we carried out structural modifications of compound **5** via an empirical medicinal chemistry approach. We first explored the influence of the substitution pattern of methoxy and vinyl groups on compound **5** (Table 1). Bromostilbene compound **9a** did not show any anti-NV activity. Compound **10a** possessing a vinyl group displayed >70% NV inhibition whereas vinyl stilbene **10b** with –OMe groups on ring B drastically decreased inhibition. Additionally, natural product mimic **11** without –OMe groups was evaluated and showed moderate inhibitory activity against NV. Furthermore, to validate the importance of the vinyl moiety on compound **5**, compounds **12a** (without a vinyl moiety) and **12b** (with an ethyl moiety) were evaluated. Of note, these compounds exhibited a distinct loss of anti-NV activity, suggesting that vinyl stilbene scaffold may be optimal for inhibitory activity against NV replication (Table 1).

Insert Table 1

Taken together with previous results, ring A was kept intact and the *para* position of ring B was explored, therefore, replacement of the -H atom at the *para* position with functional groups such as -F, -CF₃, -CO₂H, and -CO₂Me was carried out (Table 2). Compound **16a** with a fluorine atom showed moderate NV inhibition whereas a MOM ether linker (**16b**) exhibited no activity. Interestingly, introduction of a -CF₃ (**16c**) at the *para* position greatly enhanced NV inhibition (81%) with reduced toxicity. However, orienting -CF₃ to the *ortho* (**16d**) and *meta* (**16e**) positions resulted in complete loss of potency. The carboxylic acid (**16f**) and ester (**16g**) analogs were also inactive (Table 2). This vinyl stilbene series suggested that -OMe groups and a vinyl moiety on ring A and *para* substitution on ring B were critical for antiviral potency. The -CF₃ substituted vinyl stilbene **16c** was more potent, indicating that subtle structural modification could greatly improve antiviral activity. Compound **16c** afforded our first significant gain in potency and was used as a launching pad for the design and synthesis of more vinyl stilbene analogs.

Insert Table 2

Given the encouraging potency of compound **16c**, ring A was kept intact and -CF₃ was replaced with an ester motif at the *para* position of ring B. The carboxylic ester analogs **17a–d** did not significantly improve potency suggesting that incorporation of the ester linkage was detrimental to anti-NV activity (Table 3). Hence, the introduction of an amide linkage at the *para* position of ring B was envisaged and accordingly amide analogs **18a–k** were synthesized (Tables 3).

The furfuryl amine compound **18a** with one carbon linker inhibited NV replication by 66%, whereas the allylamine analog **18b** and the 4-trifluoromethyl anilide **18c** exhibited poor NV inhibitory activity. 2-Phenylethanamine compound **18d** with two carbon linkers inhibited NV by 72%. Furthermore, replacing the benzene ring of **18d** with a heterocycle (e.g. pyridine, compounds **18e** and **18f**) enhanced the NV inhibition. Both compounds **18e** and **18f** inhibited NV replication by 85% and 87% respectively, with better cell viability. The pyridine ring led to active compounds, further stressing that these groups may involve in hydrogen bonding with its target protein; however, the position of the pyridine-nitrogen atom is not a major factor for potency. Amide analogs of tyramine (**18g**) and tryptamine (**18h**) also displayed moderate NV inhibitory activity (Table 3). Based on this analysis, amide linkage with a two carbon linker and nitrogen-containing moieties are advantageous in term of potency and log P (Appendix A, Table S1). In another approach, the carbon linker was replaced with the conformationally locked piperazine motif to give compounds **18i–k** (Table 3). Among them, compound **18i** with isopropyl piperazine was found to be toxic and displayed low NV inhibitory activity, and compound **18j** with 2-(piperazine-1-yl)ethanol did not show any anti-NV activity. Interestingly, compound **18k** possessing the 1-(4-(trifluoromethyl)benzyl)piperazine moiety showed excellent inhibition of NV replication by 95.8%.

The least toxicity and highest suppressive effect of compound **18k** on virus replication prompted us to quantify the effect of substituted piperazine on anti-NV activity. Hence, a series of extended piperazine analogues were prepared in an attempt to further drive potency (Table 3, compounds **18l,m** and **24a,b**). However, in contrast to compound **18k**, compound **18l** with fluoro and **18m** with the electron donating –OMe group behaved very differently against NV replication and did not show the same degree of potency, instead resulting in increased toxicity.

Lastly, to validate the importance of *trans* geometry of potent compound **18k**, its *cis* isomer **24a** and saturated analog **24b** were synthesized. Both these compounds exhibited poor NV activity emphasizing the importance of the *trans* double bond (Table 3).

Insert Table 3

2.3 Dose-dependent Response on Cell Viability, NV Replication, and Protein Expression

The dose-dependent response of selected vinyl stilbene analogs on cell viability, NV genome replication, and protein expression is summarized in Table 4. Compound **16c** was equipotent with 2CMC having an EC₅₀ value 4.4 μM with a CC₅₀ value > 10 μM. Amide analogs **18e**, **18f**, and **18k** showed promising results, exhibiting EC₅₀ values of 2.0, 1.44, and 2.43 μM respectively; with a CC₅₀ value > 100 μM (Fig. 4A). In particular, 0.8 μM of **18k** was able to block the 50% of the neomycin phosphotransferase expression from the NV replicon in HG23 cells when treated for 5 days (Fig. 4B). Compounds **18e**, **18f**, and **18k** had higher therapeutic index (TI) (50.0, 69.0, and 41.2, respectively) than 2CMC (TI = 3.1) indicating a superior safety profile with respect to the reference compound. Among them, **18k** showed the most complete suppression of NV replication at the highest concentration (10 μM) as judged by RT-PCR and western blot analysis (Fig. 4B).

Insert Table 4

Insert Figure 4

2.4 Effects of Representative Compounds 18e, 18f, and 18k on HNV RdRp Activity

To test the potential effects of **18e**, **18f**, and **18k** on enzymatic activity of the HNV RdRp protein, we performed an *in vitro* RNA polymerase assay at 10 μ M. As shown in Fig. 5, no significant effects were detected, indicating that the antiviral activities of **18e**, **18f**, and **18k** do not depend on any direct inhibition of HNV RNA polymerase. In line with this evidence, we failed to isolate **18k**-resistant HNV genome-containing HG23 cells in the presence of escalating doses of **18k** up to 10 μ M (data not shown). This relatively high resistance barrier suggests potential targeting of host proteins by **18k** for its antiviral activity.

Insert Figure 5

2.5 Microsomal Stability of Representative Compounds 18e, 18f, and 18k

Many pharmacological compounds encounter formidable challenges to their metabolic stability *in vivo*, which is broadly considered a significant parameter in drug discovery. To assess the drug-likeness of this series of analogs, we determined the metabolic stability of the potent compounds **18e**, **18f**, and **18k** (Table 5). The *in vitro* metabolic stabilities of these analogs were examined by measuring the percentage remaining during a 30 min upon incubation with human and mouse liver microsomes in the presence of an NADPH regeneration system. Verapamil was used as a reference compound. Compound **18e** exhibited poor stability against human liver microsomes; however, it showed good stability against mouse liver microsomes in the presence of cofactor NADPH. Compound **18f** showed poor metabolic stability in human and mouse liver microsomes. In contrast, **18k** had the highest stability in both human and mouse liver microsomes in the presence of the cofactor NADPH. Moreover, no significant change was observed in the **18e**, **18f**, and **18k** concentrations during the microsomal incubations in the

absence of NADPH. Considering that metabolic stability is one of the major issues for drug development, these results merit further study of compound **18k** as a promising lead.

Insert Table 5

2.6 Effects of 18k on NV Infection Using Surrogate Infectious Models

As there is no infectious model available for HNV, we tested the potential activity of **18k** on MNV-1 and FCV which are surrogate infectious models for HNV. Compound **18k** failed to exhibit any antiviral activity against MNV-1, nevertheless, it exhibited moderate inhibition against FCV infection at concentrations $> 5 \mu\text{M}$. These data suggest that **18k** inhibits HNV replication possibly via HNV- and human cell-specific mode of actions (Fig. 6).

Insert Figure 6

2.7 Effect of 18k on Multiple Host Signal Transduction Pathways

To gain insight into the potential antiviral mechanism of action, we studied the effect of **18k** on multiple host signal transduction pathways using a commercially available 45 pathway reporter array (Table 6). As shown in Fig. 7B, both nuclear factor erythroid 2-related factor 2 (Nrf2)-dependent anti-oxidative and heat shock factor (HSF)-1-dependent stress-inducible pathways were specifically activated by **18k** treatment. This finding suggests the potential involvement of these two pathways in antiviral action of **18k**. However, neither pharmacological activation nor CRISPR-Cas9-mediated knock-out of the Nrf2 gene induced a significant effect on HNV replication, ruling out its direct causative role in **18k**-induced antiviral effects (data not shown). Interestingly, 2CMC treatment also induced the activation of HSF-1-dependent

signaling pathway (Fig. 7A). In line with this, we were also able to confirm the dose-dependent induction of HSF-1 protein by **18k** treatment (Fig. 7C). We are currently elucidating the potential role of HSF-1 in the antiviral action of **18k** in NV infection.

Insert Table 6

Insert Figure 7

Journal Pre-proof

3. Conclusions

Based on the identification of hit compound **5**, an additional series of structurally-diverse stilbenoids was synthesized and evaluated, resulting in the identification of novel NV inhibitors that inhibited NV replication in the very low μM or sub- μM range. Among the synthesized compounds, the vinyl stilbene scaffold with appended substituted amides, **18e**, **18f**, and **18k** exhibited excellent anti-NV activity with EC_{50} values of 2.0, 1.44, and 2.43 μM , respectively and TIs in the range of 40 to 70. 1-(4-(Trifluoromethyl)benzyl)piperazine amide stilbene **18k** was the least toxic displaying the highest suppressive effect on virus replication. Remarkably, compound **18k** inhibited the viral RNA genome replication in a human NV-specific manner. Multiple Host Signal Transduction pathways studies pointed towards the potential involvement of HSF-1-dependent stress-inducible pathway which was confirmed by the dose-dependent induction of HSF-1 protein with **18k** treatment. To the best of our knowledge, this is the first example of host-targeting antivirals directed against NV infection except for the deubiquitinases inhibitor, WP1130 [19]. Host-targeting nature is an advantageous approach in antiviral therapeutics as it is less likely to confer drug resistance issues; elucidation of the potential involvement of HSF-1-dependent pathway in antiviral action of these compounds may greatly facilitate the development of effective anti-NV therapeutics in the near future.

4. Experimental section

4.1 Chemistry

4.1.1 General

All the commercial chemicals were of reagent grade and were used without further purification. Reactions were conducted under an atmosphere of dried argon in flame-dried glassware. ^1H NMR spectra were determined on a Varian (400 MHz) spectrometer (Varian Medical Systems, Inc., Palo Alto, CA, USA). The ^1H NMR data are reported as peak multiplicities: s for singlet, d for doublet, dd for doublet of doublets, t for triplet, q for quartet, br for broad singlet, and m for multiplet. ^{13}C NMR spectra were recorded on a Varian (100 MHz) spectrometer. The values of the chemical shifts are expressed in δ values (ppm), and the coupling constants (J) are reported in Hertz (Hz). Mass spectra were recorded using high-resolution mass spectrometry (HRMS, ESI-MS), obtained on a G2 QTOF mass spectrometer (Waters Corp, Milford, USA). Products were purified by column or flash chromatography (Biotage, Sweden) using silica gel 60 (230–400 mesh Kieselgel 60). TLC on 0.25 mm silica plates (E. Merck; silica gel 60 F254) was used to monitor the reactions. Spots were detected by viewing under UV light and colorized with charring after dipping in anisaldehyde or basic KMnO_4 solution. The purity of the final products was checked by reversed phase high-pressure liquid chromatography (RP-HPLC), which was performed on a Waters Corp. HPLC system equipped with an ultraviolet (UV) detector set at 254 nm. The mobile phases used were (A) H_2O containing 0.05% trifluoroacetic acid and (B) CH_3CN . HPLC employed a YMC Hydrosphere C18 (HS-302) column (5 μm particle size, 12 nm pore size) that was 4.6 mm in diameter \times 150 mm in size with a flow rate of 1.0 mL/min. The compound purity was assessed using a gradient of 25% B to

100% B in 35 min. All biologically evaluated compounds purity was > 95%. Detailed synthetic procedures and spectral characterization for all intermediates are provided in the Supporting Information.

(E)-5-(3,5-Dimethoxystyryl)-2-(2-hydroxyethyl)benzene-1,3-diol [**Gramistilbenoid C (3)**].¹⁷

Compound **3** was obtained as a brown semi-solid (80.0 mg, 58% yield). ¹H NMR (methanol-*d*₄, 400 MHz) δ 6.94 (d, *J* = 16.4 Hz, 1H), 6.90 (d, *J* = 16.4 Hz, 1H), 6.65 (d, *J* = 2.4 Hz, 2H), 6.49 (s, 2H), 6.38 (t, *J* = 2.2 Hz, 1H), 3.79 (s, 6H), 3.46 (t, *J* = 8.4 Hz, 2H), 3.14 (t, *J* = 8.4 Hz, 2H); ¹³C NMR (methanol-*d*₄, 100 MHz) δ 162.5, 157.8, 140.8, 138.3, 130.3, 129.1, 113.6, 105.8, 105.4, 100.7, 55.8, 31.4, 28.9; HRMS (ESI) *m/z* calcd for C₁₈H₂₁O₅ [M + H]⁺ 317.1389, found 317.1408; RP-HPLC purity 92% at 254 nm, *t*_R = 16.48 min.

(E)-2-Bromo-5-(3,5-dimethoxystyryl)-1,3-dimethoxybenzene (**4**).¹⁷ Compound **4** was obtained as a white solid (3.90 g, 66% yield). ¹H NMR (CDCl₃, 400 MHz) δ 7.05 (d, *J* = 16.4 Hz, 1H), 7.00 (d, *J* = 16.0 Hz, 1H), 6.71 (s, 2H), 6.68 (d, *J* = 2.4 Hz, 2H), 6.42 (t, *J* = 2.4 Hz, 1H), 3.95 (s, 6H), 3.83 (s, 6H); ¹³C NMR (CDCl₃, 100 MHz) δ 161.1, 157.2, 138.8, 137.6, 129.5, 128.7, 104.7, 102.9, 100.5, 100.4, 56.5, 55.4; HRMS (ESI) *m/z* calcd for C₁₈H₂₀BrO₄ [M + H]⁺ 379.0545, found 379.0606; RP-HPLC purity 99% at 254 nm, *t*_R = 22.28 min.

(E)-5-(3,5-Dimethoxystyryl)-1,3-dimethoxy-2-vinylbenzene (**5**).¹⁷ Compound **5** was obtained as a light green solid (0.35 g, 88% yield). ¹H NMR (CDCl₃, 400 MHz) δ 7.02 (s, 2H), 6.97 (dd, *J* = 17.8, 12.2 Hz, 1H), 6.69 (s, 2H), 6.67 (d, *J* = 2.0 Hz, 2H), 6.40 (s, 1H), 6.10 (dd, *J* = 18.0, 2.8 Hz, 1H), 5.44 (dd, *J* = 12.2, 2.6 Hz, 1H), 3.90 (s, 6H), 3.83 (s, 6H); ¹³C NMR (CDCl₃, 100 MHz) δ 161.0, 158.7, 139.1, 137.2, 129.3, 128.8, 127.2, 118.5, 114.8, 104.6, 102.3, 100.2, 55.7, 55.4;

HRMS (ESI) m/z calcd for $C_{20}H_{23}O_4$ $[M + H]^+$ 327.1596, found 327.1681; RP-HPLC purity 97% at 254 nm, $t_R = 23.97$ min.

(E)-2-[4-(3,5-Dimethoxystyryl)-2,6-dimethoxyphenyl]ethanol (**6**).¹⁷ Compound **6** was obtained as a white solid (0.33 g, 72% yield). 1H NMR ($CDCl_3$, 400 MHz) δ 7.05 (d, $J = 16.4$ Hz, 1H), 6.99 (d, $J = 16.0$ Hz, 1H), 6.71 (s, 2H), 6.68 (d, $J = 2.4$ Hz, 2H), 6.40 (s, 1H), 3.88 (s, 6H), 3.84 (s, 6H), 3.77 (t, $J = 6.0$ Hz, 2H), 2.98 (t, $J = 6.6$ Hz, 2H), 1.83 (br, 1H); ^{13}C NMR ($CDCl_3$, 100 MHz) δ 161.0, 158.6, 139.2, 136.8, 129.5, 128.5, 115.3, 104.5, 102.2, 100.1, 62.8, 55.8, 55.4, 26.6; HRMS (ESI) m/z calcd for $C_{20}H_{25}O_5$ $[M + H]^+$ 345.1702, found 345.1787; RP-HPLC purity 98% at 254 nm, $t_R = 18.96$ min.

General Procedure for HWE Olefination (9a). To a solution of aryl phosphonate (1.2 equiv) in THF at 0 °C under Ar atmosphere, NaH (60% dispersion in mineral oil, 2.0 equiv) was slowly added, and the reaction was stirred for 30 min. A solution of the corresponding benzaldehyde (1.0 equiv) in THF was added dropwise and the resulting reaction mixture was stirred at rt for 12 h. The reaction was monitored by TLC. After completion of the reaction, the mixture was cooled to 0 °C and excess NaH was quenched with water. The reaction mixture was poured on ice, followed by the addition of 2.0 N HCl till pH 6 was obtained and the product was extracted with EtOAc. The combined organic layers were washed with brine, dried over $MgSO_4$, filtered, and concentrated in vacuo. Purification by Flash Column Chromatography (FCC) afforded the desired *(E)*-stilbene.

(E)-1-Bromo-4-styrylbenzene (**9a**). Purification by FCC (silica gel, 0–5% EtOAc in hexanes) afforded **9a** as a white solid (0.54 g, 30% yield). 1H NMR ($CDCl_3$, 400 MHz) δ 7.51–7.46 (m, 4H), 7.37 (d, $J = 8.8$ Hz, 4H), 7.28 (d, $J = 8.0$ Hz, 1H), 7.09 (d, $J = 16.0$ Hz, 1H), 7.02 (d, $J =$

16.4 Hz, 1H); ^{13}C NMR (CDCl_3 , 100 MHz) δ 136.9, 136.2, 131.7, 129.4, 128.7, 127.9, 127.8, 127.4, 126.5, 121.3; RP-HPLC purity 96.0% at 254 nm, $t_{\text{R}} = 25.32$ min.

General Procedure for Stille Coupling (10a,b). Tributyl(vinyl)tin (1.1 equiv), CsF (2.0 equiv), and $\text{Pd}(t\text{-Bu}_3\text{P})_2$ (0.01 equiv) were added to a solution of corresponding (*E*)-bromostilbene (1.0 equiv) in toluene and the resulting reaction mixture was refluxed for 12 h. The reaction was monitored by TLC. The solution was cooled, filtered through a celite-silica pad to remove a fine tan powder and thoroughly washed with diethyl ether. The obtained filtrate was concentrated in vacuo to give a crude product. Purification by FCC afforded the corresponding vinyl stilbene.

(E)-1-Styryl-4-vinylbenzene (**10a**). Purification by FCC (silica gel, 0–5% EtOAc in hexanes) afforded **10a** as a white solid (0.18 g, 97% yield). ^1H NMR (CDCl_3 , 400 MHz) δ 7.51 (d, $J = 7.2$ Hz, 2H), 7.48 (d, $J = 8.4$ Hz, 2H), 7.40 (d, $J = 8.4$ Hz, 2H), 7.36 (t, $J = 7.6$ Hz, 2H), 7.26 (t, $J = 7.2$ Hz, 1H), 7.10 (s, 2H), 6.72 (dd, $J = 17.6, 10.8$ Hz, 1H), 5.76 (d, $J = 17.6$ Hz, 1H), 5.25 (d, $J = 11.2$ Hz, 1H); ^{13}C NMR (CDCl_3 , 100 MHz) δ 137.3, 136.9, 136.8, 136.4, 128.7, 128.6, 128.3, 127.6, 126.7, 126.54, 126.49, 113.7; HRMS (ESI) m/z calcd for $\text{C}_{16}\text{H}_{15}$ $[\text{M} + \text{H}]^+$ 207.1174, found 207.1185; RP-HPLC purity 96.9% at 254 nm, $t_{\text{R}} = 22.33$ min.

(E)-1,3-Dimethoxy-5-(4-vinylstyryl)benzene (**10b**). Purification by FCC (silica gel, 0–4% EtOAc in hexanes) afforded **10b** as a white solid (0.27g, 65% yield). ^1H NMR (CDCl_3 , 400 MHz) δ 7.48 (d, $J = 8.0$ Hz, 2H), 7.41 (d, $J = 8.0$ Hz, 2H), 7.08 (d, $J = 16.4$ Hz, 1H), 7.03 (d, $J = 16.4$ Hz, 1H), 6.72 (dd, $J = 17.6, 10.8$ Hz, 1H), 6.68 (d, $J = 2.0$ Hz, 2H), 6.40 (s, 1H), 5.77 (d, $J = 17.6$ Hz, 1H), 5.26 (d, $J = 10.8$ Hz, 1H), 3.84 (s, 6H); ^{13}C NMR (CDCl_3 , 100 MHz) δ 160.9, 139.3, 136.9, 136.6, 136.4, 128.7, 128.5, 126.7, 126.5, 113.8, 104.5, 100.0, 55.3; HRMS (ESI) m/z calcd for

$C_{18}H_{19}O_2$ $[M + H]^+$ 267.1385, found 267.1402; RP-HPLC purity 97.2% at 254 nm, $t_R = 5.54$ min (compound purity was assessed using a gradient of 80% CH_3CN to 100% CH_3CN in 35 min).

(E)-2-(4-Styrylphenyl)ethanol (**11**). A solution of compound **10a** (50.0 mg, 0.24 mmol) in dry THF (5.0 mL) was cooled to 0 °C, and 0.5 M 9-BBN-H in THF (2.5 mL, 1.2 mmol) was added. The reaction mixture was kept in an ice bath for 30 min, and left at rt for 20 h. The reaction progress was monitored by TLC. The reaction mixture was cooled to 0 °C, and MeOH (2.0 mL) was added dropwise. When gas evolution had ceased, H_2O (2.0 mL) was added, followed by a mixture of 2.0 M NaOH (2.0 mL) and H_2O_2 (30% (w/w) in H_2O , 1.06 mL, 9.30 mmol). The ice bath was removed and the mixture was stirred vigorously at rt for 4 h. The mixture was filtered to remove the precipitate and the filtrate was diluted with EtOAc (10.0 mL). The organic layer was washed with brine, dried over $MgSO_4$, filtered, and concentrated in vacuo. The resulting residue was purified by FCC (silica gel, 0–50% EtOAc in hexanes), furnishing **11** as a white solid (30.0 mg, 55% yield). 1H NMR ($CDCl_3$, 400 MHz) δ 7.51 (d, $J = 7.6$ Hz, 2H), 7.47 (d, $J = 8.0$ Hz, 2H), 7.36 (t, $J = 7.6$, 2H), 7.24 (t, $J = 7.2$ Hz, 3H), 7.09 (s, 2H), 3.88 (t, $J = 6.6$ Hz, 2H), 2.88 (t, $J = 6.6$ Hz, 2H); ^{13}C NMR ($CDCl_3$, 100 MHz) δ 137.9, 137.3, 135.6, 129.3, 128.6, 128.3, 128.2, 127.5, 126.7, 126.4, 63.6, 38.9; HRMS (ESI) m/z calcd for $C_{16}H_{17}O$ $[M + H]^+$ 225.1279, found 225.1268; RP-HPLC purity 95.2% at 254 nm, $t_R = 16.55$ min.

Synthesis of Compounds 12a,b. The compounds were synthesized using synthetic procedure similar to **9a**.

(E)-1,2-Bis(3,5-dimethoxyphenyl)ethene (**12a**). Purification by FCC (silica gel, 0–5% EtOAc in hexanes) afforded **12a** as a white solid (20.0 mg, 62% yield). 1H NMR ($CDCl_3$, 400 MHz) δ 7.01 (s, 2H), 6.67 (d, $J = 2.4$ Hz, 4H), 6.40 (t, $J = 2.2$ Hz, 2H), 3.83 (s, 12H); ^{13}C NMR ($CDCl_3$, 100

MHz) δ 160.9, 139.0, 129.1, 104.5, 100.4, 55.3; HRMS (ESI) m/z calcd for $C_{18}H_{21}O_4$ $[M + H]^+$ 301.1440, found 301.1443; RP-HPLC purity >99% at 254 nm, t_R = 21.52 min.

(E)-5-(3,5-Dimethoxystyryl)-2-ethyl-1,3-dimethoxybenzene (**12b**). Purification by FCC (silica gel, 0–10% EtOAc in hexanes) afforded **12b** as a white solid (40.0 mg, 44% yield). 1H NMR ($CDCl_3$, 400 MHz) δ 7.05 (d, J = 16.4 Hz, 1H), 6.98 (d, J = 16.0 Hz, 1H), 6.69 (s, 2H), 6.67 (d, J = 2.4 Hz, 2H), 6.39 (t, J = 2.2 Hz, 1H), 3.87 (s, 6H), 3.83 (s, 6H), 2.66 (q, J = 7.5 Hz, 2H), 1.08 (t, J = 7.4 Hz, 3H); ^{13}C NMR ($CDCl_3$, 100 MHz) δ 160.9, 158.1, 139.3, 135.6, 129.6, 127.8, 121.0, 104.4, 102.1, 99.8, 55.7, 55.3, 16.4, 13.8; HRMS (ESI) m/z calcd for $C_{20}H_{25}O_4$ $[M + H]^+$ 329.1753, found 329.1753; RP-HPLC purity >99% at 254 nm, t_R = 25.22 min.

Synthesis of Compounds 16a–g. Compounds **16a–e** and **16g** were synthesized using synthetic procedure similar to **10a,b**.

(E)-5-(4-Fluorostyryl)-1,3-dimethoxy-2-vinylbenzene (**16a**). Purification by FCC (silica gel, 0–4% EtOAc in hexanes) afforded **16a** as a white solid (0.19 g, 94% yield). 1H NMR ($CDCl_3$, 400 MHz) δ 7.48 (dd, J = 8.4, 5.6 Hz, 2H), 7.07 (d, J = 8.8 Hz, 2H), 6.94 (m, 3H merged), 6.69 (s, 2H), 6.10 (dd, J = 18.0, 2.8 Hz, 1H), 5.44 (dd, J = 12.8, 2.4 Hz, 1H), 3.90 (s, 6H); ^{13}C NMR ($CDCl_3$, 100 MHz) δ 163.1, 161.1, 158.7, 137.1, 133.29, 133.26, 128.57, 128.54, 128.0, 127.9, 127.6, 127.1, 118.4, 115.7, 115.5, 114.6, 102.1, 55.7; HRMS (ESI) m/z calcd for $C_{18}H_{18}FO_2$ $[M + H]^+$ 285.1290, found 285.1303; RP-HPLC purity 97.3% at 254 nm, t_R = 24.86 min.

(E)-1,3-Dimethoxy-5-(4-(methoxymethoxy)styryl)-2-vinylbenzene (**16b**). Purification by FCC (silica gel, 0–5% EtOAc in hexanes) afforded **16b** as a light yellow solid (0.38 g, 79% yield). 1H NMR ($CDCl_3$, 400 MHz) δ 7.45 (d, J = 8.8 Hz, 2H), 7.07–7.01 (m, 3H), 6.96 (s, 1H), 6.95 (dd, J

= 17.2, 10.0 Hz, 1H), 6.69 (s, 2H), 6.09 (dd, $J = 18.0, 2.8$ Hz, 1H), 5.43 (dd, $J = 12.4, 2.8$ Hz, 1H), 5.19 (s, 2H), 3.90 (s, 6H), 3.49 (s, 3H); ^{13}C NMR (CDCl_3 , 100 MHz) δ 158.7, 156.9, 137.6, 131.0, 128.2, 127.7, 127.2, 127.1, 118.2, 116.4, 114.3, 102.0, 94.4, 56.0, 55.7; HRMS (ESI) m/z calcd for $\text{C}_{20}\text{H}_{23}\text{O}_4$ $[\text{M} + \text{H}]^+$ 327.1596, found 327.1605; RP-HPLC purity >99% at 254 nm, $t_{\text{R}} = 23.4$ min.

(E)-1,3-Dimethoxy-5-(4-(trifluoromethyl)styryl)-2-vinylbenzene (**16c**). Purification by FCC (silica gel, 0–3% EtOAc in hexanes) afforded **16c** as a white solid (0.77 g, 83% yield). ^1H NMR (CDCl_3 , 400 MHz) δ 7.61 (s, 4H), 7.15 (d, $J = 16.4$ Hz, 1H), 7.09 (d, $J = 16.4$ Hz, 1H), 6.98 (dd, $J = 18.0, 12.4$ Hz, 1H), 6.73 (s, 2H), 6.12 (dd, $J = 18.0, 2.8$ Hz, 1H), 5.46 (dd, $J = 12.0, 2.8$ Hz, 1H), 3.91 (s, 6H); ^{13}C NMR (CDCl_3 , 100 MHz) δ 158.7, 140.6, 136.6, 131.3, 129.5, 129.1, 127.2, 127.1, 126.6, 125.7–125.5, 118.8, 115.3, 102.5, 55.8; HRMS (ESI) m/z calcd for $\text{C}_{19}\text{H}_{18}\text{F}_3\text{O}_2$ $[\text{M} + \text{H}]^+$ 335.1259, found 335.1243; RP-HPLC purity 98.4% at 254 nm, $t_{\text{R}} = 26.62$ min.

(E)-1,3-Dimethoxy-5-(2-(trifluoromethyl)styryl)-2-vinylbenzene (**16d**). Purification by FCC (silica gel, 0–5% EtOAc in hexanes) afforded **16d** as a white solid (33.0 mg, 38% yield). ^1H NMR (CDCl_3 , 400 MHz) δ 7.78 (d, $J = 8.0$ Hz, 1H), 7.67 (d, $J = 7.6$ Hz, 1H), 7.54 (t, $J = 7.6$ Hz, 1H), 7.44 (d, $J = 16.0$ Hz, 1H), 7.36 (t, $J = 7.6$ Hz, 1H), 7.03 (d, $J = 15.6$ Hz, 1H), 6.98 (dd, $J = 18.0, 12.0$ Hz, 1H), 6.71 (s, 2H), 6.11 (dd, $J = 18.0, 2.8$ Hz, 1H), 5.46 (dd, $J = 12.0, 2.8$ Hz, 1H), 3.91 (s, 6H); ^{13}C NMR (CDCl_3 , 100 MHz) δ 158.7, 136.8, 136.2, 132.7, 131.8, 127.2, 127.1, 126.9, 126.0, 125.99, 125.93, 125.79, 124.5, 123.0, 118.7, 115.3, 102.6, 55.77, 55.74; HRMS (ESI) m/z calcd for $\text{C}_{19}\text{H}_{18}\text{F}_3\text{O}_2$ $[\text{M} + \text{H}]^+$ 335.1259, found 335.1255; RP-HPLC purity 98.3% at 254 nm, $t_{\text{R}} = 26.33$ min.

(E)-1,3-Dimethoxy-5-(3-(trifluoromethyl)styryl)-2-vinylbenzene (**16e**). Purification by FCC (silica gel, 0–5% EtOAc in hexanes) afforded **16e** as a light yellow solid (32.0 mg, 37% yield). ^1H NMR (CDCl_3 , 400 MHz) δ 7.76 (s, 1H), 7.68 (d, $J = 7.6$ Hz, 1H), 7.52–7.45 (m, 2H merged), 7.14 (d, $J = 16.8$ Hz, 1H), 7.10 (d, $J = 16.8$ Hz, 1H), 6.98 (dd, $J = 18.0, 12.4$ Hz, 1H), 6.72 (s, 2H), 6.12 (dd, $J = 18.0, 2.8$ Hz, 1H), 5.46 (dd, $J = 12.2, 2.6$ Hz, 1H), 3.91 (s, 6H); ^{13}C NMR (CDCl_3 , 100 MHz) δ 158.7, 137.9, 136.6, 131.3, 130.9, 130.6, 129.5, 129.1, 127.17, 127.10, 124.13, 124.09, 123.0, 118.7, 115.1, 102.4, 55.78, 55.75; HRMS (ESI) m/z calcd for $\text{C}_{19}\text{H}_{18}\text{F}_3\text{O}_2$ $[\text{M} + \text{H}]^+$ 335.1259, found 335.1252; RP-HPLC purity 98.5% at 254 nm, $t_{\text{R}} = 26.47$ min.

(E)-Methyl 4-(3,5-dimethoxy-4-vinylstyryl)benzoate (**16g**). Purification by FCC (silica gel, 0–4% EtOAc in hexanes) afforded **16g** as a light green solid (0.70 g, 95% yield). ^1H NMR (CDCl_3 , 400 MHz) δ 8.03 (d, $J = 8.0$ Hz, 2H), 7.58 (d, $J = 8.4$ Hz, 2H), 7.19 (d, $J = 16.0$ Hz, 1H), 7.12 (d, $J = 16.4$ Hz, 1H), 6.99 (dd, $J = 18.0, 12.0$ Hz, 1H), 6.73 (s, 2H), 6.12 (dd, $J = 18.0, 2.4$ Hz, 1H), 5.47 (dd, $J = 12.0, 2.8$ Hz, 1H), 3.93 (s, 3H), 3.92 (s, 6H); ^{13}C NMR (CDCl_3 , 100 MHz) δ 166.8, 158.7, 141.6, 136.7, 131.3, 130.0, 128.9, 127.6, 127.1, 126.3, 118.7, 115.2, 102.5, 55.7, 52.0; HRMS (ESI) m/z calcd for $\text{C}_{20}\text{H}_{21}\text{O}_4$ $[\text{M} + \text{H}]^+$ 325.1440, found 325.1448; RP-HPLC purity 98.7% at 254 nm, $t_{\text{R}} = 24.38$ min.

(E)-4-(3,5-Dimethoxy-4-vinylstyryl)benzoic acid (**16f**). Lithium hydroxide monohydrate (5.0 equiv) was added to a suspension of **16g** (1.0 equiv) in THF:H₂O:MeOH (1:1:1), and stirred at room temperature. Reaction mass was evaporated to dryness, residue was re-dissolved in water. The aqueous layer was washed with hexane, acidified with 2.0 M HCl and the precipitated solid was filtered and dried to obtain **16f** as a light green solid (0.15 g, 93% yield). ^1H NMR ($\text{DMSO-}d_6$, 400 MHz) δ 12.88 (br, 1H), 7.95 (d, $J = 8.4$ Hz, 2H), 7.72 (d, $J = 8.8$ Hz, 2H), 7.44 (d, $J =$

16.4 Hz, 1H), 7.38 (d, $J = 16.4$ Hz, 1H), 6.97 (s, 2H), 6.88 (dd, $J = 18.0, 12.0$ Hz, 1H), 6.05 (dd, $J = 18.0, 2.8$ Hz, 1H), 5.36 (dd, $J = 12.4, 2.8$ Hz, 1H), 3.87 (s, 6H); ^{13}C NMR (DMSO- d_6 , 100 MHz) δ 167.4, 158.7, 141.8, 137.5, 131.5, 130.2, 129.9, 128.3, 127.5, 126.9, 118.7, 114.1, 103.2, 56.2; HRMS (ESI) m/z calcd for $\text{C}_{19}\text{H}_{19}\text{O}_4$ $[\text{M} + \text{H}]^+$ 311.1283, found 311.1280; RP-HPLC purity 96.7% at 254 nm, $t_{\text{R}} = 19.41$ min.

General Procedure for the Synthesis of 17a–d. To a solution of corresponding carboxylic acid (1.0 equiv) in DMF at 0 °C under argon atmosphere, K_2CO_3 (2.0 equiv) was added, and the resulting mixture was stirred for 20 min. The corresponding benzyl or propargyl halide (1.1 equiv) was added and reaction mixture was stirred at rt for 12 h. The reaction mixture was quenched with water and extracted with EtOAc. The combined organic layers were washed with brine, dried over MgSO_4 , filtered, and concentrated in vacuo. Purification by FCC afforded the desired ester.

(E)-Prop-2-yn-1-yl 4-(3,5-dimethoxy-4-vinylstyryl)benzoate (17a). Purification by FCC (silica gel, 0–10% EtOAc in hexanes) afforded **17a** as a light green solid (0.11 g, 74% yield). ^1H NMR (CDCl_3 , 400 MHz) δ 8.06 (d, $J = 8.4$ Hz, 2H), 7.59 (d, $J = 8.4$ Hz, 2H), 7.19 (d, $J = 16.4$ Hz, 1H), 7.12 (d, $J = 16.4$ Hz, 1H), 6.98 (dd, $J = 18.0, 12.4$ Hz, 1H), 6.73 (s, 2H), 6.12 (dd, $J = 18.0, 2.8$ Hz, 1H), 5.46 (dd, $J = 12.0, 2.8$ Hz, 1H), 4.94 (d, $J = 2.4$ Hz, 2H), 3.91 (s, 6H), 2.53 (t, $J = 3.2$ Hz, 1H); ^{13}C NMR (CDCl_3 , 100 MHz) δ 165.5, 158.7, 142.0, 136.6, 131.5, 130.3, 128.1, 127.5, 127.1, 126.3, 118.8, 115.2, 102.5, 77.7, 75.0, 55.7, 52.4; HRMS (ESI) m/z calcd for $\text{C}_{22}\text{H}_{21}\text{O}_4$ $[\text{M} + \text{H}]^+$ 349.1440, found 349.1432; RP-HPLC purity 97.1% at 254 nm, $t_{\text{R}} = 24.61$ min.

(E)-Benzyl 4-(3,5-dimethoxy-4-vinylstyryl)benzoate (**17b**). Purification by FCC (silica gel, 0–10% EtOAc in hexanes) afforded **17b** as a white solid (35.0 mg, 68% yield). ^1H NMR (CDCl_3 , 400 MHz) δ 8.07 (d, $J = 8.4$ Hz, 2H), 7.57 (d, $J = 8.4$ Hz, 2H), 7.47–7.34 (m, 5H), 7.18 (d, $J = 16.0$ Hz, 1H), 7.11 (d, $J = 16.0$ Hz, 1H), 6.98 (dd, $J = 17.8, 12.2$ Hz, 1H), 6.73 (s, 2H), 6.12 (dd, $J = 18.0, 2.8$ Hz, 1H), 5.46 (dd, $J = 12.2, 2.6$ Hz, 1H), 5.37 (s, 2H), 3.91 (s, 6H); ^{13}C NMR (CDCl_3 , 100 MHz) δ 166.1, 158.7, 141.7, 136.6, 136.0, 131.3, 130.1, 128.8, 128.6, 128.3, 128.2, 127.6, 127.1, 126.3, 118.8, 115.1, 102.4, 66.7, 55.7; HRMS (ESI) m/z calcd for $\text{C}_{26}\text{H}_{25}\text{O}_4$ $[\text{M} + \text{H}]^+$ 401.1753, found 401.1751; RP-HPLC purity >99% at 254 nm, $t_{\text{R}} = 28.01$ min.

(E)-4-Fluorobenzyl 4-(3,5-dimethoxy-4-vinylstyryl)benzoate (**17c**). Purification by FCC (silica gel, 0–5% EtOAc in hexanes) afforded **17c** as a yellow solid (26.0 mg, 43% yield). ^1H NMR (CDCl_3 , 400 MHz) δ 8.04 (d, $J = 8.4$ Hz, 2H), 7.57 (d, $J = 8.4$ Hz, 2H), 7.45–7.42 (m, 2H), 7.17 (d, $J = 16.4$ Hz, 1H), 7.10 (d, $J = 16.4$ Hz, 1H), 7.09–7.05 (m, 2H), 6.98 (d, $J = 18.0, 12.0$ Hz, 1H), 6.72 (s, 2H), 6.12 (dd, $J = 18.0, 2.8$ Hz, 1H), 5.46 (dd, $J = 12.2, 2.6$ Hz, 1H), 5.32 (s, 2H), 3.90 (s, 6H); ^{13}C NMR (CDCl_3 , 100 MHz) δ 166.1, 158.7, 141.8, 136.6, 131.9, 131.4, 130.3, 130.2, 128.7, 127.5, 127.1, 126.3, 118.8, 115.6, 115.4, 115.2, 102.5, 65.9, 55.7; HRMS (ESI) m/z calcd for $\text{C}_{26}\text{H}_{24}\text{FO}_4$ $[\text{M} + \text{H}]^+$ 419.1659, found 419.1673; RP-HPLC purity 96.7% at 254 nm, $t_{\text{R}} = 28.23$ min.

(E)-4-(Trifluoromethyl)benzyl 4-(3,5-dimethoxy-4-vinylstyryl)benzoate (**17d**). Purification by FCC (silica gel, 0–5% EtOAc in hexanes) afforded **17d** as a yellow solid (22.0 mg, 33% yield). ^1H NMR (CDCl_3 , 400 MHz) δ 8.07 (d, $J = 8.4$ Hz, 2H), 7.66 (d, $J = 8.0$ Hz, 2H), 7.60–7.56 (m, 4H), 7.19 (d, $J = 16.4$ Hz, 1H), 7.12 (d, $J = 16.4$ Hz, 1H), 6.98 (dd, $J = 17.8, 12.2$ Hz, 1H), 6.73 (s, 2H), 6.12 (dd, $J = 18.0, 2.8$ Hz, 1H), 5.48 (dd, $J = 12.2, 2.6$ Hz, 1H), 5.42 (s, 2H), 3.92 (s,

6H); ^{13}C NMR (CDCl_3 , 100 MHz) δ 165.9, 158.7, 142.0, 140.0, 136.6, 131.6, 130.2, 128.4, 128.1, 127.5, 127.1, 126.4, 125.6, 125.5, 118.8, 115.3, 102.5, 65.7, 55.7; HRMS (ESI) m/z calcd for $\text{C}_{19}\text{H}_{18}\text{O}_3$ $[\text{M} - (\text{CF}_3\text{PhO})]^+$ 293.1178, found 293.1184; RP-HPLC purity 96.8% at 254 nm, t_{R} = 29.13 min.

General Procedure for Amide Coupling (18a–m). EDCI (1.2 equiv) and HOBt (1.2 equiv) or HATU (1.2 equiv) were added to a solution of appropriate acid (1.0 equiv), corresponding amine (1.0 equiv), and DIPEA (2.5 equiv) in DMF, and the reaction mixture was stirred at room temperature until complete consumption of the starting material. The reaction was monitored by TLC. The reaction mixture was quenched with water and extracted with EtOAc. The combined organic layer was washed with brine, dried over anhydrous MgSO_4 , and concentrated in vacuo. The resulting residue was purified by FCC.

(E)-4-(3,5-Dimethoxy-4-vinylstyryl)-N-(furan-2-ylmethyl)benzamide (18a). EDCI and HOBt were used as coupling reagents. Purification by FCC (silica gel, 0–30% EtOAc in hexanes) afforded **18a** as a white solid (28.0 mg, 45% yield). ^1H NMR (CDCl_3 , 400 MHz) δ 7.78 (d, J = 8.4 Hz, 2H), 7.56 (d, J = 8.0 Hz, 2H), 7.39 (s, 1H), 7.14 (d, J = 16.0 Hz, 1H), 7.09 (d, J = 16.4 Hz, 1H), 6.98 (dd, J = 18.0, 12.0 Hz, 1H), 6.72 (s, 2H), 6.43 (t, J = 5.4 Hz, 1H), 6.35 (s, 1H), 6.31 (s, 1H), 6.11 (dd, J = 18.0, 2.4 Hz, 1H), 5.45 (dd, J = 12.4, 2.4 Hz, 1H), 4.66 (d, J = 5.6 Hz, 2H), 3.90 (s, 6H); ^{13}C NMR (CDCl_3 , 100 MHz) δ 166.7, 158.7, 151.1, 142.3, 140.4, 136.8, 132.9, 130.9, 127.6, 127.5, 127.1, 126.5, 118.7, 115.2, 110.5, 107.7, 102.5, 55.8, 37.0; HRMS (ESI) m/z calcd for $\text{C}_{24}\text{H}_{24}\text{NO}_4$ $[\text{M} + \text{H}]^+$ 390.1705, found 390.1709; RP-HPLC purity 96.0% at 254 nm, t_{R} = 20.44 min.

(*E*)-*N*-Allyl-4-(3,5-Dimethoxy-4-vinylstyryl)benzamide (**18b**). EDCI and HOBt were used as coupling reagents. Purification by FCC (silica gel, 0–5% MeOH in DCM) afforded **18b** as a yellow solid (15.0 mg, 27% yield). ¹H NMR (CDCl₃, 400 MHz) δ 7.79 (d, *J* = 8.4 Hz, 2H), 7.57 (d, *J* = 8.4 Hz, 2H), 7.15 (d, *J* = 16.0 Hz, 1H), 7.10 (d, *J* = 16.4 Hz, 1H), 6.98 (dd, *J* = 18.0, 12.4 Hz, 1H), 6.73 (s, 2H), 6.20 (t, *J* = 5.4 Hz, 1H), 6.12 (dd, *J* = 18.0, 2.8 Hz, 1H), 6.00–5.90 (m, 1H), 5.46 (dd, *J* = 12.2, 2.6 Hz, 1H), 5.29 (dd, *J* = 17.0, 1.0 Hz, 1H), 5.21 (dd, *J* = 10.2, 1.0 Hz, 1H), 4.12 (t, *J* = 5.6 Hz, 2H), 3.91 (s, 6H); ¹³C NMR (CDCl₃, 100 MHz) δ 166.8, 158.7, 140.3, 136.7, 134.1, 133.1, 130.7, 127.5, 127.4, 127.1, 126.5, 118.7, 116.8, 115.0, 102.4, 55.7, 42.4; HRMS (ESI) *m/z* calcd for C₂₂H₂₄NO₃ [M + H]⁺ 350.1756, found 350.1746; RP-HPLC purity 95.8% at 254 nm, *t*_R = 19.93 min.

(*E*)-4-(3,5-Dimethoxy-4-vinylstyryl)-*N*-(4-(trifluoromethyl)phenyl)benzamide (**18c**). EDCI and HOBt were used as coupling reagents. Purification by FCC (silica gel, 0–20% EtOAc in hexanes) afforded **18c** as a white solid (33.0 mg, 66% yield). ¹H NMR (CDCl₃, 400 MHz) δ 7.93 (d, *J* = 8.0 Hz, 2H), 7.85 (d, *J* = 8.4 Hz, 2H), 7.64 (s, *J* = 7.4 Hz, 4H), 7.20 (d, *J* = 16.4 Hz, 1H), 7.14 (d, *J* = 16.8 Hz, 1H), 6.98 (dd, *J* = 17.8, 12.2 Hz, 1H), 6.75 (s, 2H), 6.12 (dd, *J* = 18.0, 2.4 Hz, 1H), 5.46 (dd, *J* = 12.2, 2.8 Hz, 1H), 3.92 (s, 6H), 3.38 (br, 1H); ¹³C NMR (CDCl₃, 100 MHz) δ 166.3, 158.8, 141.0, 136.8, 133.2, 131.2, 128.0, 127.5, 127.2, 126.7, 126.2, 120.1, 118.8, 115.3, 102.6, 55.8; HRMS (ESI) *m/z* calcd for C₂₆H₂₃F₃NO₃ [M + H]⁺ 454.1630, found 454.1631; RP-HPLC purity 95.3% at 254 nm, *t*_R = 26.98 min.

(*E*)-4-(3,5-Dimethoxy-4-vinylstyryl)-*N*-phenethylbenzamide (**18d**). EDCI and HOBt were used as coupling reagents. Purification by FCC (silica gel, 0–30% EtOAc in hexanes) afforded **18d** as a white solid (35.0 mg, 53% yield). ¹H NMR (CDCl₃, 400 MHz) δ 7.69 (d, *J* = 8.4 Hz, 2H), 7.54

(d, $J = 8.8$ Hz, 2H), 7.33 (d, $J = 7.2$ Hz, 2H), 7.26 (t, $J = 6.2$ Hz, 3H), 7.13 (d, $J = 16.4$ Hz, 1H), 7.08 (d, $J = 16.0$ Hz, 1H), 6.98 (dd, $J = 18.0, 12.4$ Hz, 1H), 6.71 (s, 2H), 6.11 (dd, $J = 17.8, 2.6$ Hz, 1H), 5.45 (dd, $J = 12.2$ Hz, 2.6 Hz, 1H), 3.90 (s, 6H), 3.74 (q, $J = 6.5$ Hz, 2H), 2.95 (t, $J = 6.8$ Hz, 2H); ^{13}C NMR (CDCl_3 , 100 MHz) δ 166.9, 158.7, 140.2, 138.9, 136.7, 133.3, 130.7, 128.8, 128.7, 127.6, 127.3, 127.1, 126.6, 126.5, 118.7, 115.1, 102.4, 55.7, 41.1, 35.7; HRMS (ESI) m/z calcd for $\text{C}_{27}\text{H}_{28}\text{NO}_3$ $[\text{M} + \text{H}]^+$ 414.2069, found 414.2069; RP-HPLC purity 98.4% at 254 nm, $t_{\text{R}} = 22.45$ min.

(E)-4-(3,5-Dimethoxy-4-vinylstyryl)-*N*-(2-(pyridin-4-yl)ethyl)benzamide (**18e**). EDCI and HOBT were used as coupling reagents. Purification by FCC (silica gel, 0–100% EtOAc in hexanes) afforded **18e** as a white solid (26.0 mg, 39% yield). ^1H NMR (CDCl_3 , 400 MHz) δ 8.54 (d, $J = 5.6$ Hz, 2H), 7.70 (d, $J = 8.0$ Hz, 2H), 7.56 (d, $J = 8.4$ Hz, 2H), 7.18 (d, $J = 5.6$ Hz, 2H), 7.15 (d, $J = 16.4$ Hz, 1H), 7.09 (d, $J = 16.4$ Hz, 1H), 6.98 (dd, $J = 18.0, 12.0$ Hz, 1H), 6.72 (s, 2H), 6.24 (t, $J = 5.6$ Hz, 1H), 6.12 (dd, $J = 18.0, 2.8$ Hz, 1H), 5.46 (dd, $J = 12.2, 2.6$ Hz, 1H), 3.91 (s, 6H), 3.75 (q, $J = 6.7$ Hz, 2H), 2.97 (t, $J = 7.0$ Hz, 2H); ^{13}C NMR (CDCl_3 , 100 MHz) δ 167.1, 158.7, 150.0, 148.0, 140.7, 136.7, 132.9, 130.9, 127.4, 127.3, 127.1, 126.6, 124.2, 118.7, 115.1, 102.4, 55.7, 40.3, 35.1; HRMS (ESI) m/z calcd for $\text{C}_{26}\text{H}_{27}\text{N}_2\text{O}_3$ $[\text{M} + \text{H}]^+$ 415.2022, found 415.2024; RP-HPLC purity 96.8% at 254 nm, $t_{\text{R}} = 9.68$ min.

(E)-4-(3,5-Dimethoxy-4-vinylstyryl)-*N*-(2-(pyridin-2-yl)ethyl)benzamide (**18f**). EDCI and HOBT were used as coupling reagents. Purification by FCC (silica gel, 0–5% MeOH in DCM) afforded **18f** as a light brown solid (12.0 mg, 53% yield). ^1H NMR (CDCl_3 , 400 MHz) δ 8.58 (d, $J = 4.8$ Hz, 1H), 7.79 (d, $J = 8.4$ Hz, 2H), 7.67–7.63 (m, 1H), 7.57 (d, $J = 8.4$ Hz, 3H), 7.23 (d, $J = 8.0$ Hz, 1H), 7.20–7.17 (m, 1H), 7.15 (d, $J = 16.4$ Hz, 1H), 7.10 (d, $J = 16.0$ Hz, 1H), 6.98 (dd, $J =$

18.0, 12.0 Hz, 1H), 6.72 (s, 2H), 6.11 (dd, $J = 18.0, 2.8$ Hz, 1H), 5.46 (dd, $J = 12.0, 2.8$ Hz, 1H), 3.91 (s, 6H), 3.88 (q, $J = 6.0$ Hz, 2H), 3.12 (t, $J = 6.2$ Hz, 2H); ^{13}C NMR (CDCl_3 , 100 MHz) δ 166.7, 159.9, 158.7, 149.1, 140.0, 136.8, 133.5, 130.5, 127.7, 127.4, 127.1, 126.5, 123.6, 121.7, 118.7, 115.0, 102.4, 55.7, 39.1, 36.5; HRMS (ESI) m/z calcd for $\text{C}_{26}\text{H}_{27}\text{N}_2\text{O}_3$ $[\text{M} + \text{H}]^+$ 415.2022, found 415.2022; RP-HPLC purity 98.6% at 254 nm, $t_{\text{R}} = 9.65$ min.

(E)-4-(3,5-Dimethoxy-4-vinylstyryl)-*N*-(4-hydroxyphenethyl)benzamide (**18g**). EDCI and HOBt were used as coupling reagents. Purification by FCC (silica gel, 0–5% MeOH in DCM) afforded **18g** as a light brown solid (44.0 mg, 72% yield). ^1H NMR ($\text{DMSO}-d_6$, 400 MHz) δ 9.18 (s, 1H), 8.53 (t, $J = 5.6$ Hz, 1H), 7.85 (d, $J = 8.4$ Hz, 2H), 7.69 (d, $J = 8.4$ Hz, 2H), 7.41 (d, $J = 16.8$ Hz, 1H), 7.35 (d, $J = 16.4$ Hz, 1H), 7.03 (d, $J = 8.4$ Hz, 2H), 6.95 (s, 2H), 6.89 (dd, $J = 18.0, 12.0$ Hz, 1H), 6.69 (d, $J = 8.4$ Hz, 2H), 6.05 (dd, $J = 18.0, 2.8$ Hz, 1H), 5.35 (dd, $J = 12.4, 2.8$ Hz, 1H), 3.87 (s, 6H), 3.42 (q, $J = 6.8$ Hz, 2H), 2.73 (t, $J = 7.6$ Hz, 2H); ^{13}C NMR ($\text{DMSO}-d_6$, 100 MHz) δ 165.5, 162.1, 158.2, 155.5, 139.5, 137.1, 133.3, 130.1, 129.4, 129.3, 127.9, 127.5, 126.9, 126.1, 118.0, 115.0, 113.3, 102.5, 55.6, 41.1, 35.6; HRMS (ESI) m/z calcd for $\text{C}_{27}\text{H}_{28}\text{NO}_4$ $[\text{M} + \text{H}]^+$ 430.2018, found 430.2017; RP-HPLC purity 98.9% at 254 nm, $t_{\text{R}} = 18.87$ min.

(E)-*N*-(2-(1*H*-indol-3-yl)ethyl)-4-(3,5-dimethoxy-4-vinylstyryl)benzamide (**18h**). EDCI and HOBt were used as coupling reagents. Purification by FCC (silica gel, 0–50% EtOAc in hexanes) afforded **18h** as a light yellow solid (18.0 mg, 25% yield). ^1H NMR (CDCl_3 , 400 MHz) δ 8.16 (br, 1H), 7.67 (d, $J = 8.0$ Hz, 3H), 7.52 (d, $J = 8.4$ Hz, 2H), 7.40 (d, $J = 8.0$ Hz, 1H), 7.24 (t, $J = 8.2$ Hz, 1H), 7.15 (t, $J = 7.4$ Hz, 1H), 7.12 (d, $J = 16.0$ Hz, 1H), 7.08 (d, $J = 2.4$ Hz, 1H), 7.07 (d, $J = 16.0$ Hz, 1H), 6.98 (dd, $J = 18.0, 12.4$ Hz, 1H), 6.71 (s, 2H), 6.23 (t, $J = 5.6$ Hz, 1H), 6.11 (dd, $J = 18.0, 2.4$ Hz, 1H), 5.46 (dd, $J = 12.2, 2.6$ Hz, 1H), 3.91 (s, 6H), 3.82 (q, $J = 6.4$ Hz, 2H),

3.12 (t, $J = 6.4$ Hz, 2H); ^{13}C NMR (CDCl_3 , 100 MHz) δ 166.9, 158.6, 140.0, 136.7, 136.3, 133.3, 130.2, 127.5, 127.3, 127.0, 126.4, 122.3, 122.1, 119.6, 118.8, 118.7, 114.9, 113.4, 111.2, 102.3, 55.7, 40.2, 25.2; HRMS (ESI) m/z calcd for $\text{C}_{29}\text{H}_{29}\text{N}_2\text{O}_3$ $[\text{M} + \text{H}]^+$ 453.2178, found 453.2182; RP-HPLC purity 98.1% at 254 nm, $t_{\text{R}} = 21.72$ min.

(E)-(4-(3,5-Dimethoxy-4-vinylstyryl)phenyl)(4-isopropylpiperazin-1-yl)methanone (**18i**). HATU was used as a coupling reagent. Purification by FCC (silica gel, 0–100% EtOAc in hexanes) afforded **18i** as a pale yellow viscous solid (8.0 mg, 15% yield). ^1H NMR (CDCl_3 , 400 MHz) δ 7.53 (d, $J = 8.0$ Hz, 2H), 7.41 (d, $J = 8.0$ Hz, 2H), 7.08 (s, 2H), 6.98 (dd, $J = 18.2, 12.2$ Hz, 1H), 6.70 (s, 2H), 6.11 (dd, $J = 18.0, 2.8$ Hz, 1H), 5.44 (dd, $J = 12.0, 2.8$ Hz, 1H), 3.89 (s, 6H), 3.78 (br, 2H), 3.47 (br, 2H), 2.75–2.69 (m, 1H), 2.57 (br, 2H), 2.47 (br, 2H), 1.05 (d, $J = 6.8$ Hz, 6H); ^{13}C NMR (CDCl_3 , 100 MHz) δ 169.9, 158.7, 138.5, 136.9, 134.7, 130.1, 127.76, 127.71, 127.1, 126.4, 118.5, 114.9, 102.4, 55.74, 55.71, 54.5, 49.0, 48.3, 48.1, 42.5, 18.3; HRMS (ESI) m/z calcd for $\text{C}_{26}\text{H}_{33}\text{N}_2\text{O}_3$ $[\text{M} + \text{H}]^+$ 421.2491, found 421.2478; RP-HPLC purity 97.8% at 254 nm, $t_{\text{R}} = 10.05$ min.

(E)-(4-(3,5-Dimethoxy-4-vinylstyryl)phenyl)(4-(2-hydroxyethyl)piperazin-1-yl)methanone (**18j**). HATU was used as a coupling reagent. Purification by FCC (silica gel, 0–5% MeOH in DCM) afforded **18j** as a white solid (36.0 mg, 53% yield). ^1H NMR (CDCl_3 , 400 MHz) δ 7.55 (d, $J = 8.0$ Hz, 2H), 7.41 (d, $J = 8.0$ Hz, 2H), 7.12 (d, $J = 16.4$ Hz, 1H), 7.08 (d, $J = 17.2$ Hz, 1H), 6.98 (dd, $J = 18.0, 12.4$ Hz, 1H), 6.72 (s, 2H), 6.11 (dd, $J = 18.0, 2.4$ Hz, 1H), 5.46 (dd, $J = 12.2, 2.6$ Hz, 1H), 3.91 (s, 6H), 3.81 (br, 2H), 3.66 (t, $J = 5.2$ Hz, 2H), 3.52 (br, 2H), 2.60 (t, $J = 5.2$ Hz, 2H), 2.53 (br, 4H); ^{13}C NMR (CDCl_3 , 100 MHz) δ 170.0, 158.7, 138.7, 136.8, 134.5, 130.2, 127.7, 127.1, 126.4, 118.6, 115.0, 102.4, 59.3, 57.7, 55.7, 53.2, 52.6, 47.7, 42.0; HRMS (ESI)

m/z calcd for $C_{25}H_{31}N_2O_4$ $[M + H]^+$ 423.2284, found 423.2275; RP-HPLC purity 96.2% at 254 nm, $t_R = 8.79$ min.

(E)-(4-(3,5-Dimethoxy-4-vinylstyryl)phenyl)(4-(4-(trifluoromethyl)benzyl)piperazin-1-yl)methanone (**18k**). HATU was used as a coupling reagent. Purification by FCC (silica gel, 0–70% EtOAc in hexanes) afforded **18k** as a light yellow solid (51.0 mg, 59% yield). 1H NMR ($CDCl_3$, 400 MHz) δ 7.58 (d, $J = 8.0$ Hz, 2H), 7.54 (d, $J = 8.0$ Hz, 2H), 7.46 (d, $J = 8.0$ Hz, 2H), 7.41 (d, $J = 8.4$ Hz, 2H), 7.11 (d, $J = 16.4$ Hz, 1H), 7.07 (d, $J = 16.8$ Hz, 1H), 6.97 (dd, $J = 18.0$, 12.0 Hz, 1H), 6.71 (s, 2H), 6.11 (dd, $J = 18.0$, 2.4 Hz, 1H), 5.45 (dd, $J = 12.0$, 2.8 Hz, 1H), 3.91 (s, 6H), 3.78 (br, 2H), 3.59 (s, 2H), 3.50 (br, 2H), 2.49 (br, 4H); ^{13}C NMR ($CDCl_3$, 100 MHz) δ 170.0, 158.7, 141.9, 138.6, 136.9, 134.7, 130.2, 129.7, 129.4, 129.1, 127.8, 127.7, 127.1, 126.4, 125.4–125.2, 118.6, 115.1, 102.4, 62.3, 55.8, 53.0, 52.9, 47.7, 42.2; HRMS (ESI) m/z calcd for $C_{31}H_{32}F_3N_2O_3$ $[M + H]^+$ 537.2365, found 537.2372; RP-HPLC purity 96.6% at 254 nm, $t_R = 12.78$ min.

(E)-(4-(3,5-Dimethoxy-4-vinylstyryl)phenyl)(4-(4-fluorobenzyl)piperazin-1-yl)methanone (**18l**). HATU was used as a coupling reagent. Purification by FCC (silica gel, 0–70% EtOAc in hexanes) afforded **18l** as a white solid (26.0 mg, 55% yield). 1H NMR ($CDCl_3$, 400 MHz) δ 7.54 (d, $J = 8.0$ Hz, 2H), 7.41 (d, $J = 8.0$ Hz, 2H), 7.29 (dd, $J = 8.0$, 5.2 Hz, 2H), 7.11 (d, $J = 16.4$ Hz, 1H), 7.07 (dd, $J = 16.8$ Hz, 1H), 7.03–6.94 (m, 3H), 6.71 (s, 2H), 6.11 (dd, $J = 18.0$, 2.8 Hz, 1H), 5.45 (dd, $J = 12.2$, 2.6 Hz, 1H), 3.91 (s, 6H), 3.79 (br, 2H), 3.50 (s, 2H), 3.48 (br, 2H), 2.51 (br, 2H), 2.39 (br, 2H); ^{13}C NMR ($CDCl_3$, 100 MHz) δ 170.0, 163.3, 160.8, 158.7, 138.6, 136.8, 134.7, 133.2, 130.6, 130.5, 130.1, 127.7, 127.1, 126.4, 118.6, 115.2, 115.0, 102.3, 62.0, 55.7,

53.2, 52.7, 47.8, 42.2; HRMS (ESI) m/z calcd for $C_{30}H_{32}FN_2O_3$ $[M + H]^+$ 487.2397, found 487.2397; RP-HPLC purity 99.2% at 254 nm, $t_R = 12.36$ min.

(E)-(4-(3,5-Dimethoxy-4-vinylstyryl)phenyl)(4-(4-methoxybenzyl)piperazin-1-yl)methanone

(18m). HATU was used as a coupling reagent. Purification by FCC (silica gel, 0–70% EtOAc in hexanes) afforded **18m** as a light green solid (34.0 mg, 70% yield). 1H NMR ($CDCl_3$, 400 MHz) δ 7.54 (d, $J = 8.4$ Hz, 2H), 7.40 (d, $J = 8.4$ Hz, 2H), 7.23 (d, $J = 8.8$ Hz, 2H), 7.11 (d, $J = 16.8$ Hz, 1H), 7.07 (d, $J = 16.4$ Hz, 1H), 6.98 (dd, $J = 18.0, 12.4$ Hz, 1H), 6.86 (dd, $J = 8.8$ Hz, 2H), 6.71 (s, 2H), 6.11 (dd, $J = 18.0, 2.8$ Hz, 1H), 5.45 (dd, $J = 12.2, 2.6$ Hz, 1H), 3.91 (s, 6H), 3.80 (s, 3H), 3.78 (br, 2H), 3.48 (s, 2H), 3.46 (br, 2H), 2.52 (br, 2H), 2.39 (br, 2H); ^{13}C NMR ($CDCl_3$, 100 MHz) δ 169.9, 158.8, 158.7, 138.5, 136.8, 134.7, 130.3, 130.1, 129.4, 127.8, 127.7, 127.1, 126.4, 118.6, 114.9, 113.6, 102.3, 62.2, 55.7, 55.2, 53.2, 52.6, 47.7, 42.0; HRMS (ESI) m/z calcd for $C_{31}H_{35}N_2O_4$ $[M + H]^+$ 499.2597, found 499.2597; RP-HPLC purity 97.3% at 254 nm, $t_R = 12.31$ min.

(Z)-(4-(3,5-Dimethoxy-4-vinylstyryl)phenyl)(4-(4-(trifluoromethyl)benzyl)piperazin-1-

yl)methanone (24a). The compound was synthesized using synthetic procedure similar to **18a–m** using HATU as a coupling reagent. Purification by FCC (silica gel, 0–70% EtOAc in hexanes) afforded **24a** as a white solid (29.0 mg, 33% yield). 1H NMR ($CDCl_3$, 400 MHz) δ 7.58 (d, $J = 8.4$ Hz, 2H), 7.45 (d, $J = 8.4$ Hz, 2H), 7.33 (d, $J = 8.0$ Hz, 2H), 7.29 (d, $J = 8.0$ Hz, 2H), 6.92 (dd, $J = 18.0, 12.4$ Hz, 1H), 6.61 (d, $J = 12.8$ Hz, 1H), 6.58 (d, $J = 13.2$ Hz, 1H), 6.43 (s, 2H), 6.06 (dd, $J = 18.0, 2.8$ Hz, 1H), 5.42 (dd, $J = 12.0, 2.8$ Hz, 1H), 3.77 (br, 2H), 3.64 (s, 6H), 3.57 (s, 2H), 3.42 (br, 2H), 2.51 (br, 2H), 2.37 (br, 2H); ^{13}C NMR ($CDCl_3$, 100 MHz) δ 169.9, 158.2, 141.8, 138.9, 136.6, 134.2, 131.4, 129.5, 129.1, 129.0, 127.1, 127.0, 125.3–125.2, 118.5, 114.0,

104.5, 62.2, 55.5, 53.2, 52.7, 47.6, 42.1; HRMS (ESI) m/z calcd for $C_{31}H_{32}F_3N_2O_3$ $[M + H]^+$ 537.2365, found 537.2365; RP-HPLC purity >99% at 254 nm, $t_R = 12.48$ min.

(4-(3,5-Dimethoxy-4-vinylphenethyl)phenyl)(4-(4-(trifluoromethyl)benzyl)piperazin-1-yl)methanone (24b). The compound was synthesized using synthetic procedure similar to **18a–m** using HATU as a coupling reagent. Purification by FCC (silica gel, 0–70% EtOAc in hexanes) afforded **24b** as a white solid (85.0 mg, 98% yield). 1H NMR ($CDCl_3$, 400 MHz) δ 7.58 (d, $J = 8.4$ Hz, 2H), 7.45 (d, $J = 8.4$ Hz, 2H), 7.32 (d, $J = 8.4$ Hz, 2H), 7.20 (d, $J = 7.6$ Hz, 2H), 6.93 (dd, $J = 18.0, 12.4$ Hz, 1H), 6.32 (s, 2H), 6.02 (dd, $J = 18.0, 2.8$ Hz, 1H), 5.39 (dd, $J = 12.4, 2.8$ Hz, 1H), 3.79 (s, 6H), 3.79 (br, 2H merged), 3.58 (s, 2H), 3.44 (br, 2H), 2.96–2.92 (m, 2H), 2.89–2.80 (m, 2H), 2.52 (br, 2H), 2.38 (br, 2H); ^{13}C NMR ($CDCl_3$, 100 MHz) δ 170.3, 158.4, 143.4, 141.9, 133.3, 129.7, 129.4, 129.1, 128.6, 127.2, 125.31, 125.28, 122.8, 117.7, 112.7, 104.1, 62.3, 55.7, 53.4, 52.8, 47.7, 42.1, 38.2, 37.5; HRMS (ESI) m/z calcd for $C_{31}H_{34}F_3N_2O_3$ $[M + H]^+$ 539.2521, found 539.2522; RP-HPLC purity >99% at 254 nm, $t_R = 12.48$ min.

4.2 Cytotoxicity Assays

HG23 cells were plated onto a 96-well plate (Costar) and treated with DMSO or compound at 10 μ M. After 3 days, compound cytotoxicity was measured by using EZ-CYTOX (10% tetrazolium salt; Dogen) reagent.

4.3 Quantitative Real-Time-RT-PCR (qRT-PCR) Analysis

HG23 cells were plated onto a 6 well plate (Costar) with either DMSO or the compound of interest (10 μ M). After 3 days, total cellular RNA was extracted using the RNeasy®mini kit (Qiagen) according to the manufacturer's protocol. The expression of HNV subgenomic RNA

and cellular RNA was quantified through quantitative real-time reverse-transcription polymerase chain reaction (qRT-PCR) analysis as previously described. Each sample was normalized by the endogenous reference gene glyceraldehydes-3-phosphate dehydrogenase (GAPDH). The cDNA quantification was performed by the CFX384 real-time PCR detection system (Bio-Rad, US). FW-hNV- CGCTGGATGCGNTTCCATGA, RV-hNV-CTTAGA CGCCATCATCATTTAC, FW-GAPDH-TGGTCTCCTCTGACTTCA, and RV-GAPDH-CGTTGTCATACCAGGAAATG.

4.4 Western Blot Analysis

HG23 cells were plated onto a 6 well plate (Costar) and supplemented with either DMSO or an increasing concentration of the compound of interest. At 3 days after incubation, whole-cell extracts were prepared in RIPA buffer (150 mM NaCl, 1 % Triton X-100, 1 % deoxycholic acid sodium salt, 0.1 % sodium dodecyl sulfate, 50 mM Tris-HCl, 2 mM EDTA, pH 7.5; genDEPOT) containing a cocktail of Complete protease inhibitors (Roche) and quantitated by the Bradford assay (Bio-Rad). Equal amounts of protein were electrophoresed on an SDS-polyacrylamide gel, subsequently transferred to a polyvinylidene difluoride membrane (Immobilon-P; Millipore), and probed with either a rabbit anti-neomycin phosphotransferase (1:500 dilution, ab33595, Abcam) or anti-HSF-1 antibodies (1:1000 dilution, D3L8I, Cell Signaling).

4.5 MNV-1 and FCV Infection Assays

For MNV-1 infection, RAW 264.7 Cells were plated onto 12-well plate at a cell density of 0.4×10^6 cells per well. The next day, cells were infected with MNV-1 (1×10^5 PFU/well) for 1 h at 37 °C and were covered with 2 ml/well of 3% SeaPlaque agarose overlay medium containing the compound (0.05-10 μ M). After 48 h, cells were stained with 0.5% crystal violet

for 1 h at room temperature. For FCV infection, CRFK cells were plated onto 12-well plate at a cell density of 0.4×10^6 cells per well. The next day, cells were infected with FCV (1×10^6 PFU/well) for 1 h at 37 °C and were covered with 2 ml/well of 3% SeaPlaque agarose overlay medium containing the compound (0.05-10 μ M). After 48 h, cells were stained with 0.5% crystal violet for 1 h at room temperature.

4.6 Cignal Finder Reporter Array Analyses

Cignal finder reporter array analyses were performed on transfected HG23 cells using Cignal finder reporter array (CCA-901L; Qiagen) according to the manufacturer's instructions. Transfected HG23 cells were supplemented with DMSO or 10 μ M of **18k** for 72 h. Luciferase activities were measured using a luciferase reagent (The Dual-Luciferase® Reporter; Promega).

4.7 Quantitative RdRp Assays

To test Non-Nucleoside Inhibitors (NNI) Quantitative RdRp activity assays were performed with human norovirus GII.4 Sydney 2012 recombinant RdRp (Genbank accession number: KT239579) in 384-well plates, as described previously [20]. A single 25- μ L reaction mixture contained 400 ng enzyme, 5 μ M rGTP, 6 μ g/mL poly(C) RNA, 2.5 mM MnCl₂, 5 mM DTT, 0.01% bovine serum albumin (BSA), and 0.005% Tween 20 in 20 mM Tris-HCl (pH 7.5). The RdRp was incubated for 10 min at 25 °C in the presence of the test compounds or the compound vehicle DMSO (0.5% v/v) before addition into the reaction mixture. The reaction was then allowed to proceed for 15 min at 25 °C. The reaction was terminated with 10 mM EDTA, followed by PicoGreen staining and dsRNA quantitation using a POLARstar plate reader at standard wavelengths (excitation 480 nm, emission 520 nm). The compounds were assessed at a

fixed concentration of 10 μM and the average and standard deviations of two independent experiments with triplicate datasets are shown.

4.8 Microsomal Stability Studies

These studies have been performed by Anthem Biosciences according to their protocols using diclofenac and imipramine as reference compounds.

a) Sample Treatment

Two types of liver microsomes (Human and Mouse, 0.5 mg/ml), 0.1 M phosphate buffer (pH 7.4), corresponding compounds were added at a concentration of 1 μM and pre-incubated at 37 $^{\circ}\text{C}$ for 5 minutes, then NADPH regeneration system solution was added or not added and incubated at 37 $^{\circ}\text{C}$ for 30 minutes. To terminate the reaction, an acetonitrile solution containing an internal standard (chlorpropamide) was added and centrifuged (14,000 rpm, 4 $^{\circ}\text{C}$) for 5 minutes. The supernatant was injected into the LC-MS/MS system. The metabolism stability of the four compounds was evaluated by analyzing the substrate drug.

b) LC-MS/MS Analysis

The amount of substrate remaining through the reaction was determined using the Shimadzu Nexera XR system and TSQ vantage (Thermo). The HPLC column Kinetex C18 column (2.1 x 100 mm, 2.6 μm particle size; Phenomenex) was used. The mobile phase contained 0.1% formic acid in (A) distilled water and (B) acetonitrile. For data analysis, Xcalibur (version 1.6.1) was used.

Acknowledgments

This work was supported by the National Research Foundation of Korea (NRF) grant funded by the Ministry of Education, Korea government (MSIT) (No. 2018R1A5A2023127 and 2016R1D1A1B03933100).

Appendix A. Supplementary data

Supplementary data to this article can be found online at

Author information

Corresponding Authors

*Choogho Lee, Ph.D., Phone: +82-31-961-5223; E-mail: choongholee@dongguk.edu

*Kyeong Lee, Ph.D., Phone: +82-31-961-5214; E-mail: kaylee@dongguk.edu

Author Contributions

The manuscript was written through the contributions of all authors. All authors have given approval to the final version of the manuscript. The authors declare no competing financial interest.

Abbreviations

9-BBN-H, 9-borabicyclo[3.3.1]nonane; DCM, dichloromethane; DMF, dimethylformamide; DMSO, dimethyl sulfoxide; EDC, 1-ethyl-3-(3-dimethylaminopropyl)carbodiimide; EDTA, ethylenediaminetetraacetic acid; EtOAc, ethyl acetate; HATU, hexafluorophosphate azabenzotriazole tetramethyl uronium; HOBt, hydroxybenzotriazole; NADPH, nicotinamide

adenine dinucleotide phosphate; RdRp, RNA-dependent RNA polymerase; TBAI, tetrabutylammonium iodide; THF, tetrahydrofuran; TLC, thin layer chromatography.

References

- [1] S.G. Morillo, Mdo.C. Timenetsky, Norovirus: an overview, *Rev. Assoc. Med. Bras.* 57 (2011) 453–458.
- [2] K. Bok, K.Y. Green, Norovirus gastroenteritis in immunocompromised patients, *N. Engl. J. Med.* 367 (2012) 2126–2132.
- [3] H.L. DuPont, Acute infectious diarrhea in immunocompetent adults, *N. Engl. J. Med.* 370 (2014) 1532–1540.
- [4] M.de Graaf, J.van Beek, M.P. Koopmans, Human Norovirus transmission and evolution in a changing world, *Nat. Rev. Microbiol.* 14 (2016) 421–433.
- [5] <https://www.cdc.gov/norovirus/index.html> (accessed 25 June 2019).
- [6] L.G. Thorne, I.G. Goodfellow, Norovirus gene expression and replication, *J. Gen. Virol.* 95 (2014) 278–291.
- [7] M.E. Hardy, Norovirus protein structure and function, *FEMS Microbiol. Lett.* 253 (2005) 1–8.
- [8] B.V. Prasad, S. Shanker, Z. Muhaxhiri, L. Deng, J.M. Choi, M.K. Estes, Y. Song, T. Palzkill, R.L. Atmar, Antiviral targets of human noroviruses, *Curr. Opin. Virol.* 18 (2016) 117–125.

- [9] J. Rocha-Pereira, M.S. Nascimento, Q. Ma, R. Hilgenfeld, J. Neyts, D. Jochmans, The enterovirus protease inhibitor rupintrivir exerts cross-genotypic anti-norovirus activity and clears cells from the norovirus replicon, *Antimicrob. Agents Chemother.* 58 (2014) 4675–4681.
- [10] J. Rocha-Pereira, D. Jochmans, Y. Debing, E. Verbeken, M.S.J. Nascimento, J. Neyts, The viral polymerase inhibitor 2'-C-methylcytidine inhibits Norwalk virus replication and protects against norovirus-induced diarrhea and mortality in a mouse model, *J. Virol.* 87 (2013) 11798–11805.
- [11] V.P. Costantini, T. Whitaker, L. Barclay, D. Lee, T.R. McBrayer, R.F. Schinazi, J. Vinje, Antiviral activity of nucleoside analogues against norovirus, *Antiviral. Ther.* 17 (2012) 981–991.
- [12] R. Croci, M. Pezzullo, D. Tarantino, M. Milani, S.-C. Tsay, R. Sureshbabu, Y.-J. Tsai, E. Mastrangelo, J. Rohayem, M. Bolognesi, J.R. Hwu, Structural bases of norovirus RNA dependent RNA polymerase inhibition by novel suramin related compounds, *PLoS One* 9 (2014) e91765.
- [13] <http://ir.chimerix.com/news-releases/news-release-details/chimerix-announces-discovery-and-demonstrated-preclinical> (accessed 25 June 2019).
- [14] J.F. Rossignol, Y.M. El-Gohary, Nitazoxanide in treatment of viral gastroenteritis: A randomized, double-blind, placebocontrolled clinical trial, *Aliment. Pharmacol. Ther.* 24 (2006) 1423–1430.

- [15] D.M. Siddiq, H.L. Koo, J.A. Adachi, G.M. Viola, Norovirus gastroenteritis successfully treated with nitazoxanide, *J. Infect.* 63 (2011) 394–397.
- [16] M. Yang, G. Lee, J. Si, S.J. Lee, H.J. You, G. Ko, Curcumin shows antiviral properties against norovirus, *Molecules* 21 (2016) 1401.
- [17] D.S. Harmalkar, Q. Lu, K. Lee, Total synthesis of gramistilbenoids A, B, and C, *J. Nat. Prod.* 81 (2018) 798–805.
- [18] M. Numata, A. Sato, R. Nogami, Energy-dissipative self-assembly driven in microflow: A time-programmed self-organization and decomposition of metastable nanofibers, *Chem. Lett.* 44 (2015) 995–997.
- [19] J.W. Perry, M. Ahmed, K.O. Chang, N.J. Donato, H.D. Showalter, C.E. Wobus, Antiviral activity of small molecule deubiquitinase inhibitor occurs via induction of the unfolded protein response, *PLoS Pathog.* 8 (2012) e1002783.
- [20] A.A. Eltahla, K. Lackovic, C. Marquis, J.S. Eden, P.A. White, A fluorescence-based high-throughput screen to identify small compound inhibitors of the genotype 3a hepatitis C virus RNA polymerase, *J. Biomol. Screen.* 18 (2013) 1027–1034.

Figures

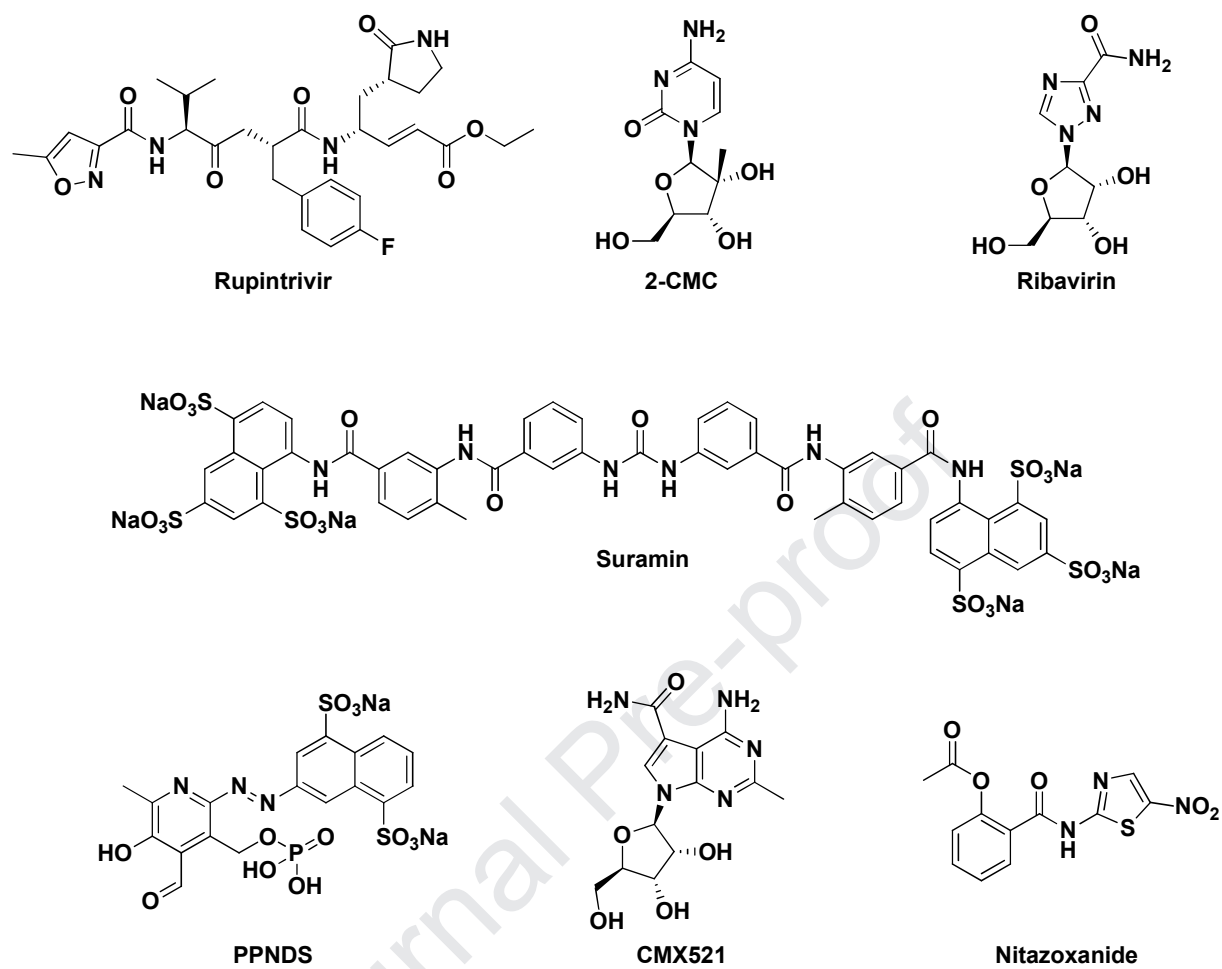


Fig. 1. Structure of reported NV inhibitors [Protease (NS6) - rupintrivir; RdRP (NS7) - 2CMC, ribavirin; suramin, and PPNDS].

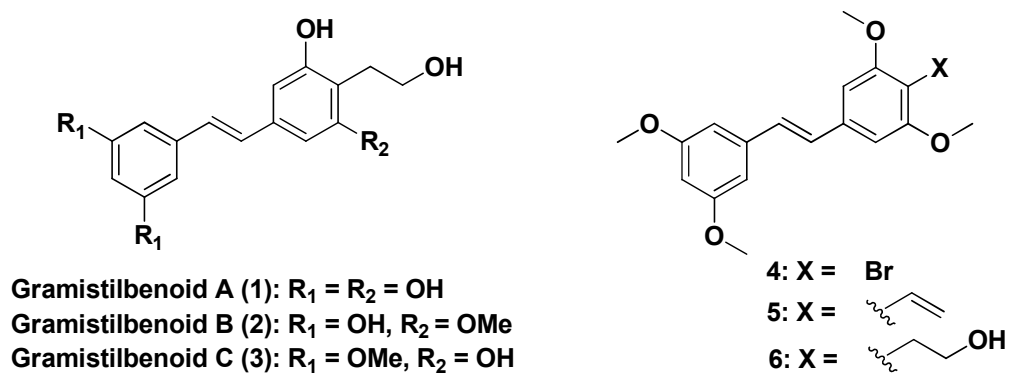


Fig. 2. Structure of gramistilbenoids A-C and compounds 4-6.

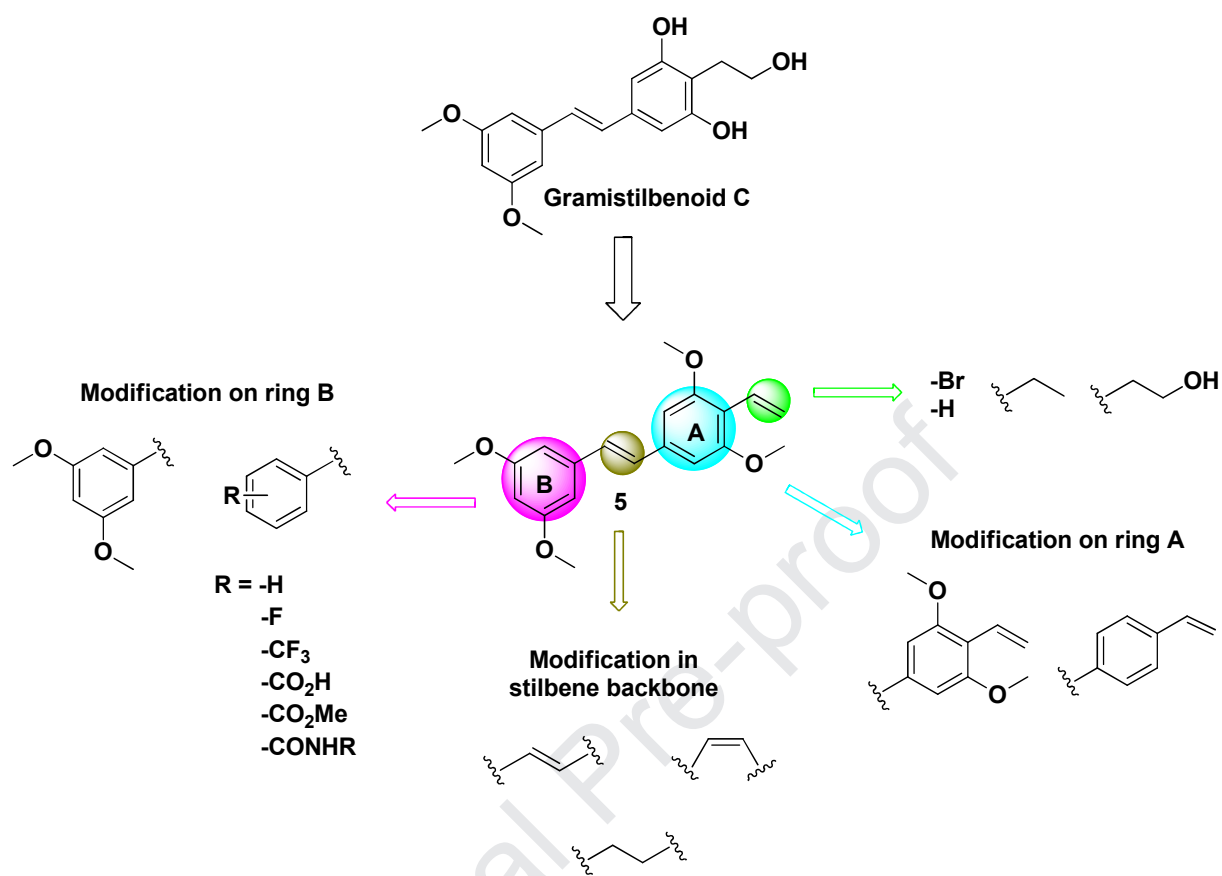
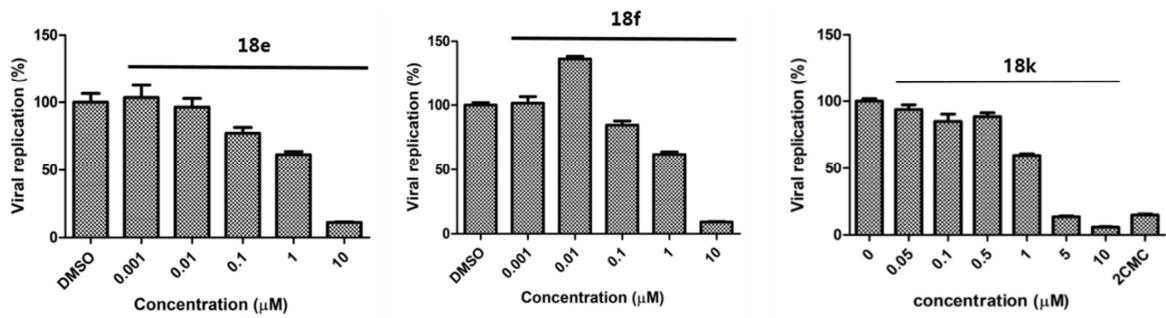


Fig. 3. An overview of SAR study on gramistilbenoids.

A



B

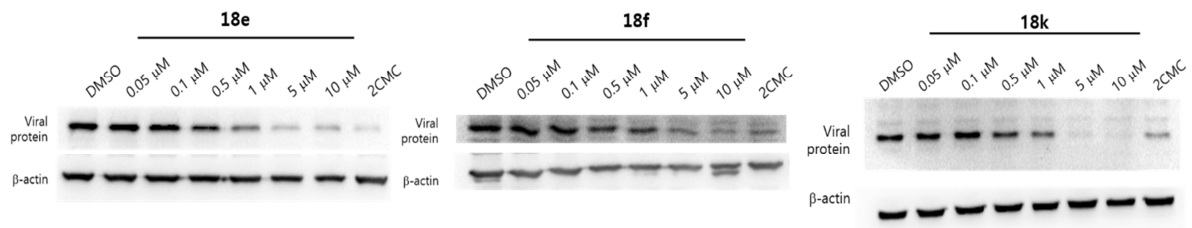


Fig. 4. Dose-dependent effects of **18e**, **18f**, and **18k** on (A) HNV replication; (B) HNV viral protein expression.

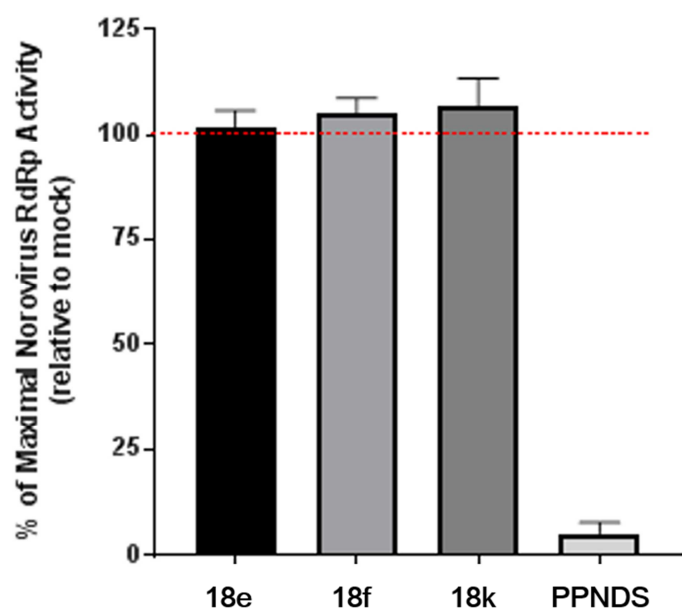


Fig. 5. Effects of the representative compounds **18e**, **18f**, and **18k** on HNV RdRp activity at 10 μ M. PPNDS was used as a positive control.

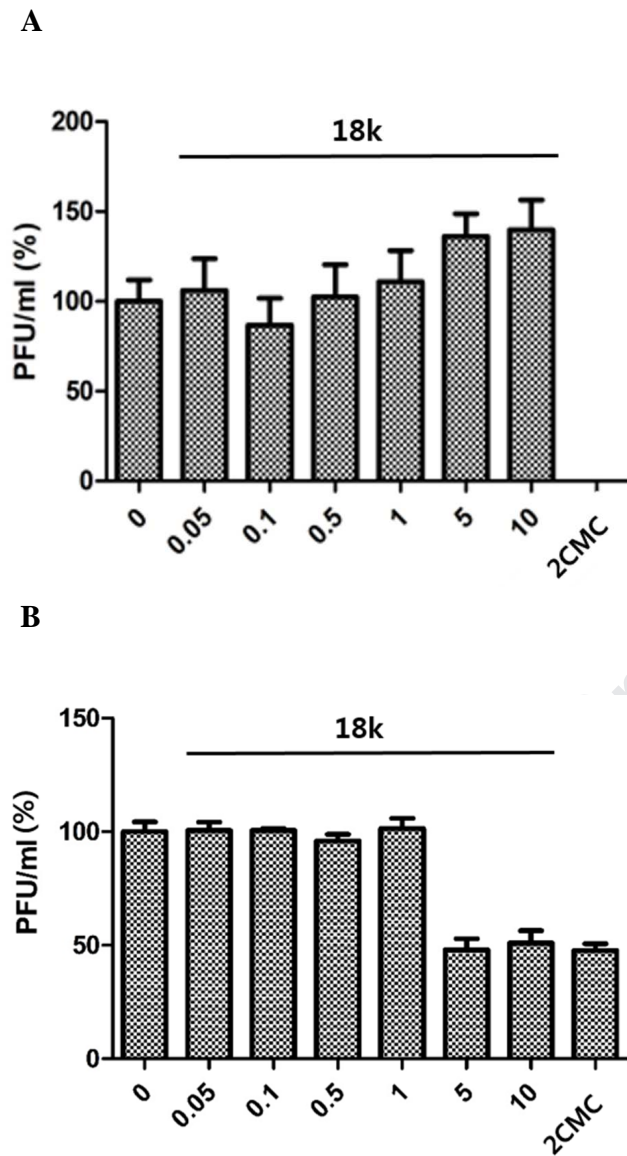
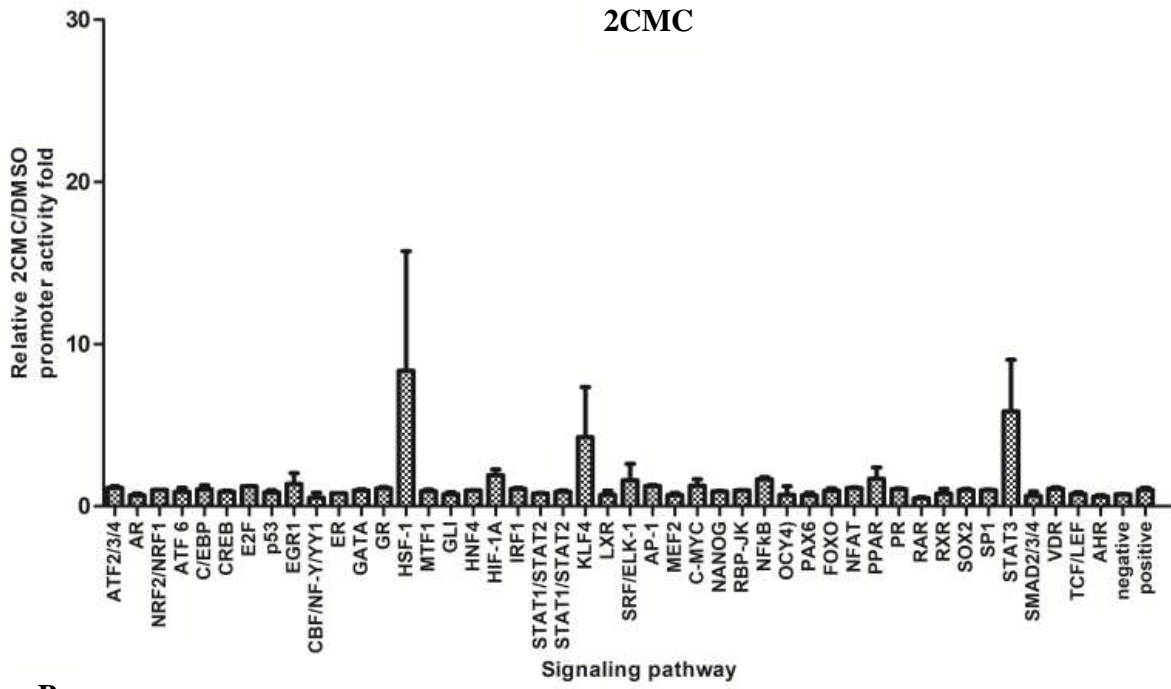
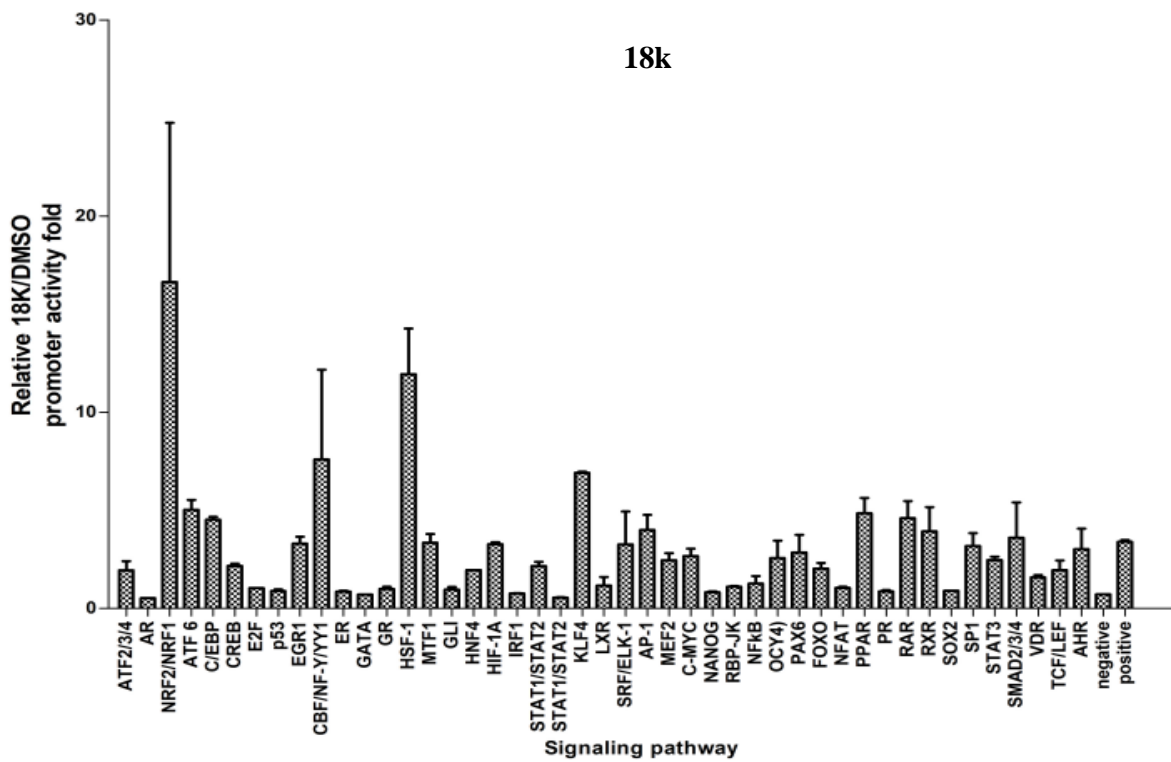


Fig. 6. Dose-dependent effects of **18k** on (A) MNV-1 and (B) FCV infections.

A



B



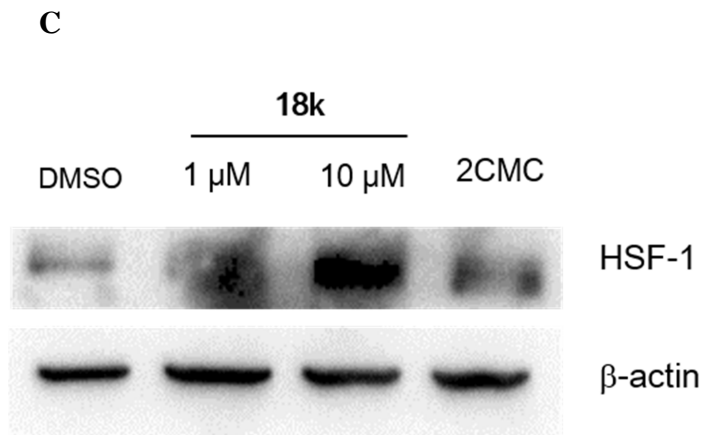
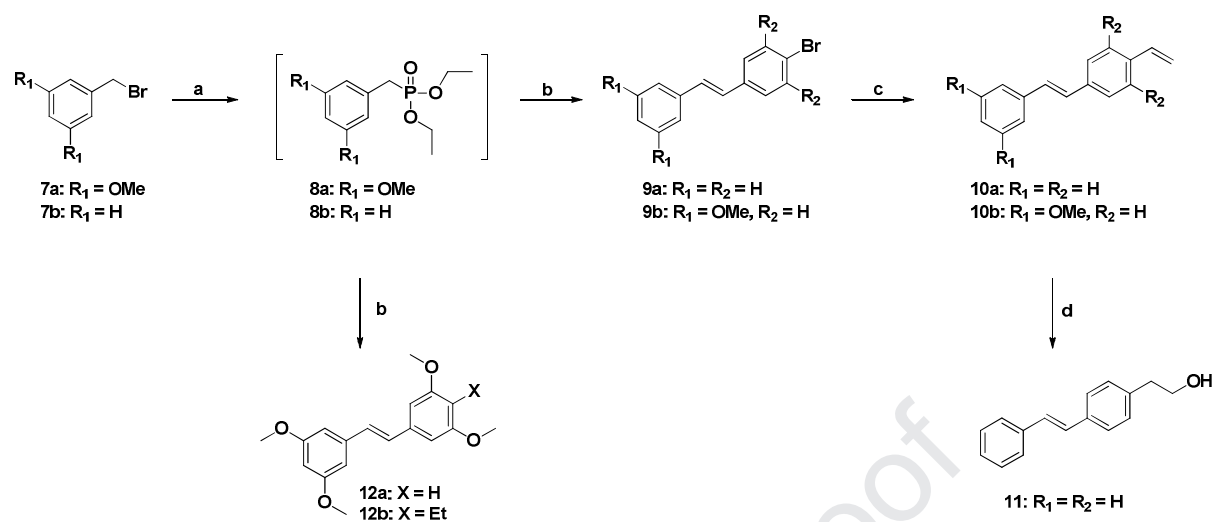


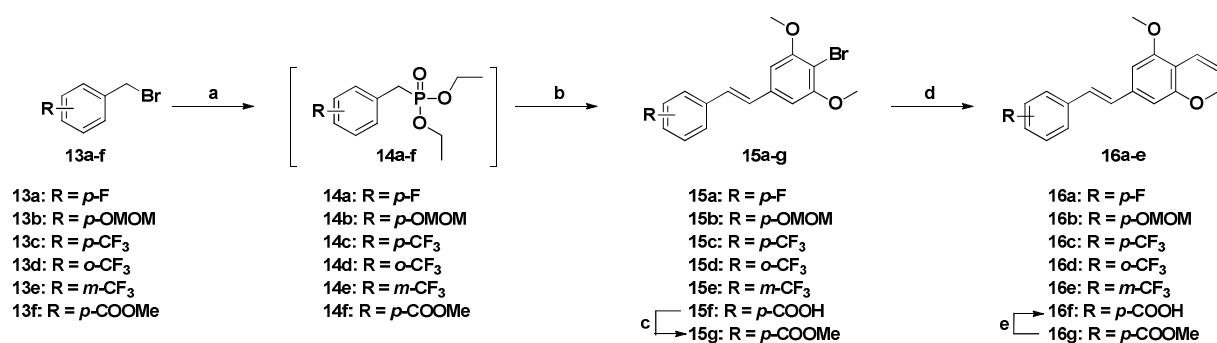
Fig. 7. Activation of HSF-1 stress-inducible pathways by **18k**. Effect of (A) 2CMC and (B) **18k** on multiple host signal transduction pathways. (C) Induction of HSF-1 protein by **18k** treatment in HG23.

Schemes

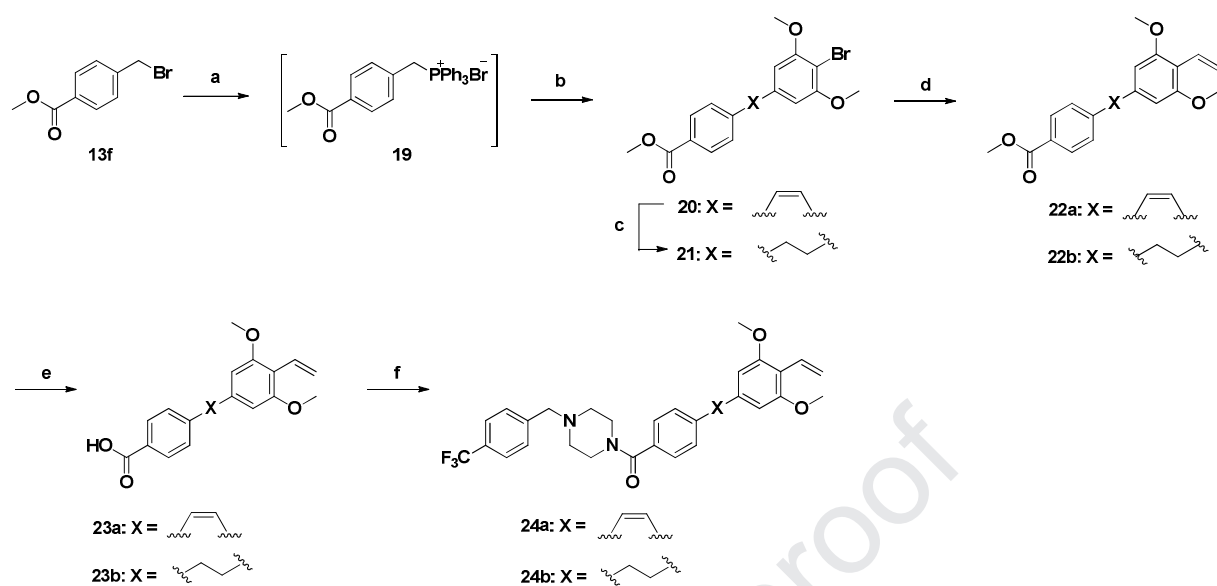
Journal Pre-proof



Scheme 1. Synthesis of Stilbenes **9a,b**; **10a,b**; **11** and **12a,b**. Reagents and Conditions: (a) P(OEt)₃, TBAI, 130 °C, 6 h; (b) 4-bromo-3,5-dimethoxybenzaldehyde for **9a,b** / 3,5-dimethoxybenzaldehyde for **12a** / 4-ethyl-3,5-dimethoxybenzaldehyde for **12b** (Appendix A, Scheme S1), NaH, THF, rt, 12 h; (c) tributyl(vinyl)tin, CsF, Pd(*t*-Bu₃P)₂, toluene, 110 °C, 12 h; (d) 0.5 M 9-BBN-H in THF, H₂O₂, 2.0 M NaOH, THF, 24 h.



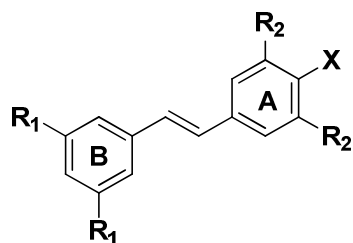
Scheme 2. Synthesis of Vinyl Stilbenes **16a–g**. Reagents and Conditions: (a) P(OEt)₃, TBAI, 130 °C, 6 h; (b) 4-bromo-3,5-dimethoxybenzaldehyde, NaH, THF, rt, 12 h; (c) MeI, K₂CO₃, DMF, rt, 12 h; (d) tributyl(vinyl)tin, CsF, Pd(*t*-Bu₃P)₂, toluene, 110 °C, 12 h; (e) LiOH, THF:H₂O:MeOH (1:1:1), rt, 12 h.



Scheme 4. Synthesis of *cis*-Analog **24a** and Saturated Analog **24b**. Reagents and Conditions: (a) PPh_3 , toluene, $110\text{ }^\circ\text{C}$; (b) 4-bromo-3,5-dimethoxybenzaldehyde, NaH , DCM ; (c) H_2 , Pd/C , EtOAc , 12 h; (d) tributyl(vinyl)tin, CsF , $\text{Pd}(t\text{-Bu}_3\text{P})_2$, toluene, $110\text{ }^\circ\text{C}$, 12 h; (e) LiOH , $\text{THF:H}_2\text{O:MeOH}$ (1:1:1), rt, 12 h; (f) 1-[4-(Trifluoromethyl)benzyl]piperazine, HATU , DIPEA , DMF , rt, 48 h.

Tables

Journal Pre-proof

Table 1In Vitro Inhibition of Norovirus Replication (Compounds **3–6**, **9a**, **10a,b**, **11**, and **12a,b**)^a.

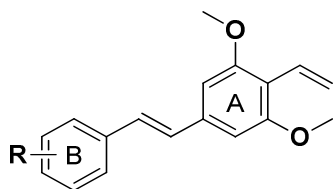
Comp	R ₁	R ₂	X	NV replication	Cell viability
				(10 μM) (%)	(10 μM) (%)
3	OMe	OH		200.8 ± 22.7	99.0 ± 0.4
4	OMe	OMe	Br	184.9 ± 6.2	99.7 ± 0.6
5	OMe	OMe		43.4 ± 1.2	99.6 ± 0.8
6	OMe	OMe		272.8 ± 10.5	99.8 ± 0.8
9a	H	H	Br	54.5 ± 5.7	130.2 ± 4.8
10a	H	H		26.5 ± 4.2	102.3 ± 0.4
10b	OMe	H		77.1 ± 20.5	138.1 ± 1.4
11	H	H		43.2 ± 4.5	100.6 ± 16.9
12a	OMe	OMe	H	119.0 ± 17.6	99.2 ± 12.3

12b	OMe	OMe		94.0 ± 15.6	69.3 ± 4.7
2CMC^b				24.8 ± 2.4	78.5 ± 0.9

^a Values are means of the most representative triplicate experiment with standard deviations.

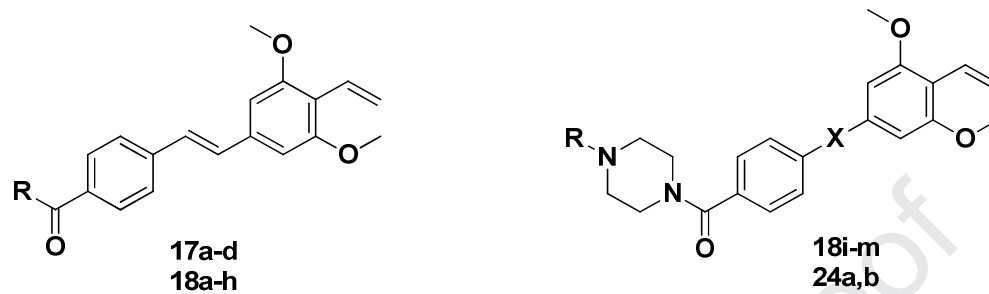
^b Reference compound.

Journal Pre-proof

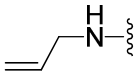
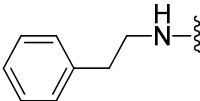
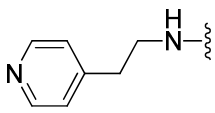
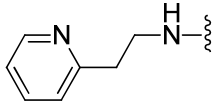
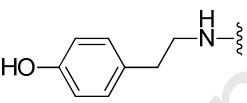
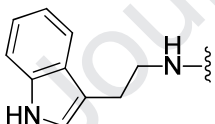
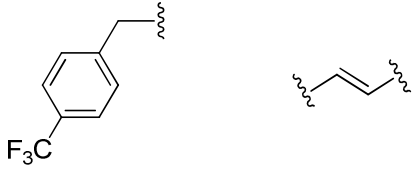
Table 2In Vitro Inhibition of Norovirus Replication (Compounds **16a–g**)^a.

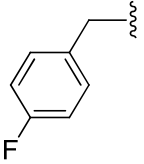
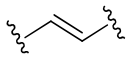
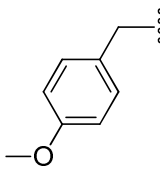
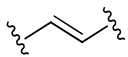
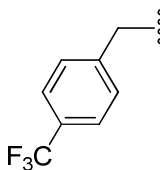
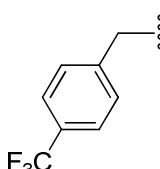
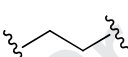
Comp	R	NV replication	Cell viability
		(10 μ M) (%) (STDEV)	(10 μ M) (%) (STDEV)
16a	<i>p</i> -F	38.4 \pm 0.7	93.2 \pm 5.1
16b	<i>p</i> -OMOM	165.7 \pm 1.2	97.5 \pm 3.5
16c	<i>p</i> -CF ₃	19.4 \pm 3.1	97.5 \pm 4.9
16d	<i>o</i> -CF ₃	83.2 \pm 27.7	99.7 \pm 13.4
16e	<i>m</i> -CF ₃	66.6 \pm 8.4	98.4 \pm 12.6
16f	<i>p</i> -COOH	81.3 \pm 2.3	111.7 \pm 9.8
16g	<i>p</i> -COOMe	58.2 \pm 6.5	110.9 \pm 17.7

^a Values are means of the most representative triplicate experiment with standard deviations.

Table 3In Vitro Inhibition of Norovirus Replication (Compounds **17a–d**, **18a–m**, and **24a,b**)^a.

Comp	R	X	NV replication	Cell viability
			(10 μ M) (%) (STDEV)	(10 μ M) (%) (STDEV)
17a		---	71.3 \pm 1.3	102.7 \pm 9.4
17b		---	134.9 \pm 5.7	105.9 \pm 14.2
17c		---	36.0 \pm 2.0	101.0 \pm 5.2
17d		---	58.4 \pm 6.7	109.2 \pm 4.0
18a		---	33.8 \pm 1.2	108.6 \pm 2.2

18b		---	62.4 ± 0.7	91.6 ± 2.8
18c		---	70.8 ± 1.2	92.5 ± 1.1
18d		---	28.4 ± 3.1	99.7 ± 1.5
18e		---	15.4 ± 0.7	100.2 ± 0.7
18f		---	13.5 ± 2.2	96.3 ± 3.5
18g		---	40.8 ± 6.7	102.6 ± 2.2
18h		---	46.6 ± 1.2	105.5 ± 2.5
18i			55.3 ± 9.2	60.5 ± 0.9
18j			110.4 ± 21.0	93.3 ± 4.1
18k			4.2 ± 0.2	105.1 ± 0.2

18l			12.1 ± 5.2	55.7 ± 5.2
18m			30.4 ± 2.2	21.5 ± 3.1
24a			64.9 ± 5.6	90.9 ± 11.6
24b			132.1 ± 3.1	77.3 ± 3.1

^a Values are means of the most representative triplicate experiment with standard deviations.

Table 4

Dose-dependent Response on Viability, Replication, and Viral Protein Expression of Representative Compounds^a.

Comp	Dose-dependent response on cell viability and NV replication		Therapeutic index CC ₅₀ /EC ₅₀	Dose-dependent response on viral protein expression EC ₅₀ (μM)
	CC ₅₀ (μM)	EC ₅₀ (μM)		
16c	> 10	4.4	> 2.2	8.0
18e	> 100	2.0	> 50	0.71
18f	> 100	1.44	> 69	1.97
18k	> 100	2.43	> 41.2	0.8
2CMC^b	12.2	4.0	3.1	4.8

^a Values are means of the most representative triplicate experiment.

^b Reference compound.

Table 5Liver Microsomal Stability Assay^a.

Comp	Metabolic Stability Assay			
	Human (%)		Mouse (%)	
	(+) NADPH	(-) NADPH	(+) NADPH	(-) NADPH
18e	20.0	92.1	67.7	88.4
18f	44.1	> 100	38.3	83.1
18k	89.1	94.3	70.5	99.2
Verapamil	13.6	-	-	-

^a % Remaining during 30 min.

Table 6

List of Signal Pathway.

NO.	Pathway	Symbol
1	Amino Acid Deprivation	ATF2/3/4
2	Androgen	AR
3	Antioxidant Response	NRF2/NRF1
4	ATF6	ATF 6
5	C/EBP	C/EBP
6	cAMP/PKA	CREB
7	Cell Cycle	E2F
8	DNA Damage	p53
9	Early Growth Response	EGR1
10	ER Stress	CBF/NF-Y/YY1
11	Estrogen Receptor	ER
12	GATA	GATA
13	Glucocorticoid Receptor	GR
14	Heat Shock Response	HSF-1
15	Heavy Metal Response	MTF1
16	Hedgehog	GLI
17	epatocyte Nuclear Factor	HNF4
18	Hypoxia	HIF-1A
19	Interferon Regulation	IRF1
20	Interferon Type I	STAT1/STAT2
21	Interferon Gamma	STAT1/STAT2
22	KLF4	KLF4
23	Liver X Receptor	LXR
24	MAPK/ERK	SRF/ELK-1
25	MAPK/JNK	AP-1
26	MEF2	MEF2
27	c-Myc	C-MYC
28	Nanog	NANOG

29	NFκB	RBP-JK
30	Notch	NFκB
31	Oct4	OCY4)
32	Pax6	PAX6
33	PI3K/AKT	FOXO
34	PKC/Ca ⁺⁺	NFAT
35	PPAR	PPAR
36	Progesterone	PR
37	tinoic Acid Receptor	RAR
38	etinoid X Receptor	RXR
39	Sox2	SOX2
40	SP1	SP1
41	STAT3	STAT3
42	TGFβ	SMAD2/3/4
43	Vitamin D	VDR
44	Wnt	TCF/LEF
45	Xenobiotic	AHR
46	Cignal Negative Control (LUC)	A mixture of non-inducible firefly luciferase reporter construct and constitutively expressing Renilla luciferase construct (40:1).
47	Cignal Positive Control	A mixture of a constitutively expressing GFP construct, constitutively expressing firefly luciferase construct, and constitutively expressing Renilla luciferase element (40:1:1).

Highlights

- A series of novel vinyl-stilbenes derivatives were designed and synthesized.
- Following a structure-activity relationship study, compound **18k** with 1-(4-(trifluoromethyl)benzyl)piperazine moiety demonstrated an excellent therapeutic index.
- Compound **18k** inhibited the viral RNA genome replication in a human NV-specific manner with EC₅₀ of 2.43 μM.
- The dose-dependent induction of HSF-1 protein on **18k** treatment strongly suggests potential involvement of HSF-1-dependent stress-inducible pathway in anti-viral action.